



*Physics of Ice, Climate and Earth
Niels Bohr Institute,
University Of Copenhagen*



*Master of Science in
Geologia e Geologia Tecnica
at the University of Padova
Geoscience department
Head master: Fabrizio Nestola*

**ATMOSPHERIC METHANE: DISCRETE
MEASUREMENTS FOR INDIVIDUAL
GREENLAND ICE CORE SAMPLES VIA THE
PICARRO G1301 ANALYZER**

Supervisor: Prof. **Thomas Blunier**
Co-supervisor: PhD **Jesper Baldtzer Liisberg**
Inner supervisor: Prof. **Luca Capraro**
Prof. **Patrizia Ferretti**

Student: **Elena Zanola**
Student number: **1178993**

Academic year: 2018-2019

*« Ultimately, it's not what you get or even what you give
It's what you become. »*

Mary Maxwell Gates

*To my parents,
and to my grandmothers Esterina and Luigia*

List of Figures

Figure 2. 1 The graph shows globally-averaged, monthly mean atmospheric methane abundance determined from marine surface sites. Particularly it represents the full NOAA times-series starting in 1983. https://www.esrl.noaa.gov/gmd/ccgg/trends_ch4/ . According to this curve, it is clearly evident the huge increasing trend which will reach the value of about 1850 ppb in the 2020, against the 1600 ppb or so of the 1980s. - 24 -

Figure 2. 2 Three dimensional representation of the latitudinal distribution of atmospheric CH₄ in the marine boundary layer, from the US National Oceanic and Atmospheric Administration, Earth System Research Laboratory, Global Monitoring Division (NOAA/ESRL/GMD) programme. Data from the Carbon Cycle cooperative global air sampling network have been used. - 28 -

Figure 2. 3 Inner view of a GC in which the capillary column is wound in a spiral around the metal support. In the upper part it is shown the injector (on the left) and the detector (on the right). - 29 -

Figure 2. 4 Two different overview of Greenland with the location of the sites for each expedition. - 31 -

Figure 2. 5 Main expeditions in Greenland in red dots - 33 -

Figure 3. 1 Picarro analyzer - 35 -

Figure 3. 2 Picarro G1301 from a laboratory view. - 35 -

Figure 3. 3 Light intensity decay path in the chamber without sample (blue) or with sample (green). - 37 -

Figure 3. 4 Principle of cavity ring down measurements top left: the beam from a single-frequency laser diode enters the cavity. Top right: the light in the cavity

rings down where the ring down time depends on the presence of the absorbing gas. Bottom: The detector signal during the measurements.	- 38 -
Figure 3. 5 DAS and PVU compartments	- 40 -
Figure 3. 6 Screen shot of the GUI user interface of the analyzer	- 41 -
Figure 3. 7 Simple scheme of the complete inner structure of the analyzer	- 42 -
Figure 3. 8 Inner disposition of the component into the DAS	- 43 -
Figure 3. 9 High finesse optical cavity	- 43 -
Figure 3. 10 Shows a cross-section through the standard sample cell with the gas inlet (in) and outlet (out) represented as black dashed circles	- 44 -
Figure 4. 1 Laboratory station: Picarro analyzer on the left and the extraction line on the background	- 48 -
Figure 4. 2 Hi-cube turbo pump	- 50 -
Figure 4. 3 Initial sequence of valves along the extraction line. In the upper central part:the digital screen of the Pressure gauge.	- 51 -
Figure 4. 4 The latest configuration of the extraction line with additional valves: S and P	- 51 -
Figure 4. 5 The flow inlet_2 represents the actual signal from the flow meter. This is converted into a flow, by fitting the voltage reading with the flow readings from a second flow meter. In fact, plotting flow inlet (ml/min) versus the flow inlet_2 is a perfect fit, as they are related by a linear fit by design. The upper graph shows the measurements taken by the external flowmeter. It provides the equation for the recalibration of the analyzer flow meter (which measurements are shown in the lower graph). The inner flowmeter is not from the Picarro manufactory but it is a Honeywell	- 53 -
Figure 4. 6 Sample trap between valve 3 (on the right) and valve 4 (on the left)	- 59 -

Figure 4. 7 Sample trap with the high resistance wire wrapped around the tube
- 60 -

Figure 4. 8 Whole view of the heating system mounted around the sample trap. The blue container helps to keep the heat and accelerate the temperature increasing.
- 60 -

Figure 4. 9 In red squares is shown the methane trend while in blue squares the carbon dioxide trend. Both of them with the respective linear equation. - 63 -

Figure 4. 10 Shows the best linear fit between inverse flow + offset and methane concentration. It is represented by the line: $y = 0,0231x + 2,1215$ - 65 -

Figure 5. 1 Methane values from continuous flow experiments with the three standards plotting against the respective expected values - 68 -

Figure 5. 2 Carbon dioxide values from continuous flow experiments with the three standards plotting against the respective expected values - 69 -

Figure 5. 3 The curve shows one of the many attempt for these kind of experiments. From the left to the right is showed the respective experiment for each standard. Black arrows indicate the introduction of the standard gas sample, followed by fifty minutes monitoring and by an evacuation (except for the last standard, where the experiment has been directly interrupted after the monitoring). - 72 -

Figure 5. 4 The anomalous trends for both CO₂ and CH₄ are showed above, as result of one of the many attempts for AFI experiments. The experiment was interrupted due to unreliable values. - 75 -

Figure 5. 5 The final calibration for real samples, based on the last Blank experiment with three standards. - 76 -

Figure 5. 6 Red curve shows the measurements from the last AFI experiment, in which the concentrations increased till stabilizing around a constant value over time; Green curve show the values with final calibration. - 77 -

Figure 5. 7 Calibration made in order to have an idea about the uncertainty of the system. It was derived on the basis of the three last Blank experiments, the best ones - 77 -

Figure 6. 1 View from the huge freezer ice storage in Prioparken - 79 -

Figure 6. 2 Another view of the ice boxes's piles. - 79 -

Figure 6. 3 A picture of me cutting the ice stick. - 80 -

Figure 6. 4 An example of ice sample sizes. - 80 -

Figure 6. 5 Standard 1 in blue dots and standard 2 in red squares, monitored everyday for daily calibration. - 81 -

Figure 6. 6 Ethanol-dry ice bath under the glass vessel - 83 -

Figure 6. 7 view of the whole extraction line during the ice melting and the extraction of the air sample. - 84 -

Figure 6. 8 An example of real sample monitoring. This is the case of sample n° 478. - 85 -

Figure 7. 1 Methane record from Eurocore ice samples both from published data and my results. In blue Bern's results, in green Grenoble's values, both measured by gas chromatography; in red squares my values, taken through the Picarro G1301 analyzer. - 90 -

Figure 8. 1 Measured values are plotted versus published values making a linear comparison. I excluded the three outliers in order to have a better fit. The relation is quite good, especially for Bern values. - 91 -

List of Tables

- Table 1** The following table shows in detail some of the specific parameters which characterized the analyser
(https://www.picarro.com/assets/docs/CO2_CH4_flightanalyzer_datasheet.pdf) - 45 -
- Table 2** Name of components employed in the experimental set up - 48 -
- Table 3** Compressed air composition for CH₄ and CO₂ - 52 -
- Table 4** Cavity pressure with respective flow and concentrations of CO₂, CH₄ and H₂O - 62 -
- Table 5** The three tests' measurements. It is evident the control of the flow on the methane concentrations. It is not the same for carbon dioxide (which explanation is possible recalling the memory effect of the sample trap) - 64 -
- Table 6** Known compositions for standard 1, standard 2 and compressed air. For the compressed air I have considered the values measured at 140 Torr, because at that pressure condition the values were certainly correct. - 67 -
- Table 7** measured values for standard 1, standard 2 and compressed air. - 67 -
- Table 8** Each sample with the respective age (years AD), depth (m) and weight (g) - 81 -
- Table 9** Standard daily measurements before the first sample of the day - 82 -
- Table 10** The measurement result from Eurocore ice samples. The depth and Gas age are provided by (Blunier et al. 1993). The variance for my measurements can be derived from the standard deviation, and is equal to 16 ppbv. - 87 -
- Table 11** The measurements results from Blunier analysis in 1993, with respective depth and Gas age. In red are shown the most deviant values compared to my measurements. The variance for Blunier's measurements is 20 ppbv. - 88 -

Table 12 The measurement results from Grenoble analysis in 1993, with respective depth and Gas age. In red are shown the most deviant values compared to my measurements. The variance for Grenoble's measurements is ± 40 ppbv.

- 89 -

List of Acronyms

cc cubic centimetre

CH₄ methane

CO₂ Carbon Dioxide

CRDS Cavity Ring Down spectrometry

DAS Data acquisition system

FID Flame Ionization Detector

GC Gas Chromatography

GUI Graphical User Interface

IPCC Intergovernmental Panel on Climate Change

mBar millibar

MS Mass Spectrometry

ppbv particles per billion by volume

ppm particles per million

PVU Power vacuum unit

SS stainless steel

TDC Thermal Conductivity Detector

Contents

1. Introduction	- 19 -
2. Background	- 23 -
2.1 Methane studies and extraction techniques	- 23 -
2.2 Methane as greenhouse gas	- 26 -
.....	- 28 -
2.3 Methane measurements techniques from ice cores	- 29 -
2.4 Brief history of ice cores drilling	- 30 -
2.5 Drilling in Greenland	- 33 -
2.6 Eurocore project	- 34 -
3. Analyzer structure and components	- 37 -
3.1 Cavity Ring-Down Spectroscopy (CRDS)	- 37 -
3.2 Theoretical background: the optical absorption and the “ring-down” time	- 38 -
3.3 The Analyzer description	- 42 -
4. Experimental set up and calibration tests	- 49 -
4.1 Experimental set up and component description	- 50 -
4.2 Development of the experiments on the set up	- 54 -
4.2.1 Re-calibration of the analyser flow meter	- 54 -
4.2.2 Preliminary experiments procedure	- 56 -
4.3 Challenges in developing the experimental set up	- 57 -
4.3.1 Presence of leaks	- 57 -
4.3.2 “Memory effect” of the sample trap	- 61 -
4.3.3 Cavity pressure	- 63 -
5. Standard calibration	- 69 -
5.1 Calibration experiments	- 72 -
5.1.1 Blank experiments	- 72 -
5.1.2 Air Free Ice (AFI) experiments	- 74 -
5.2 Analytical accuracy	- 79 -
6. Real sample experiments	- 81 -

6.1 Cutting the ice.....	- 81 -
6.2 Daily calibration	- 83 -
6.3 Real procedure	- 84 -
7. Results from Eurocore samples.....	- 89 -
7.1 Comparison with published results.....	- 89 -
8. Discussion	- 93 -
9. Conclusions	- 97 -
10. Acknowledgments.....	- 101 -
11. References	- 106 -

Abstract

Methane (CH_4) is considered the second most important greenhouse gas after carbon-dioxide (CO_2), i.e. the second major anthropogenic climate forcing contributor. Its atmospheric concentration in ancient times can be directly reconstructed on the basis of air bubbles entrapped within the ice, analysing their chemical composition. For years, at least until 2009, traditional methods for methane measurements relied on Gas Chromatography (GC) and Mass-Spectrometry (MS). Since further, new advanced techniques as Cavity Ring Down Spectrometry (CRDS) improved the analytical instrumentation and procedure, providing faster analysis and a high accuracy even with very low concentrations (ppbv). Different extraction techniques (wet, dry and sublimation), as well as sampling methods (discrete, semi-continuous and continuous), have been implemented over time, providing an even greater resolution and reliability of measurements. The continuous method allows the highest resolution, however it cannot fully compete in the reproducibility with discrete methods, particularly due to its restriction with number of samples.

I present a discrete method, developed through the Picarro G1301 analyser, to measure methane concentrations from trapped air bubbles within ice samples. These ice samples derive from the Eurocore project ice core, drilled in Central Greenland (1989) and cover a time period of about 1000 years, between 1907 and 974 AD. The results confirm the atmospheric methane record published by Blunier et al. in 1993, with a pre-industrial methane level around 700 ppbv and an anthropogenic methane increase between 1750 and 1800, which most likely matches with the dawn of the industrialization. Noteworthy is the fact that, due to the complexity of the flow effect encountered during the experiments, my values are still affected by its presence. Nevertheless, since it is incorporated in all measurements, including those of standards, it can be considered as constant and therefore neglected here. For more precise and accurate measurements a reliable flow correction must be further investigated.

1. Introduction

Over the past decades huge progress has been made in understanding how the climate system works. Particularly over the last two decades a variety of methods and instruments for measuring gases have been explored. In the frame of this thesis I worked with laser spectroscopy which has many advantages over other methods. The process of investigating climate evolution is not only important for shedding light on past climate changes but also to provide new relevant information concerning their evolution in the future. Fortunately, nature yields us many different means to work on, such as sea and lake sediments, their depositional features, seawater composition, microfossils, tree rings, pollens, ice cores, etc..

Among these means, it is the study of ice cores from glaciers or polar ice sheets which represents one of the most powerful instruments for the reconstruction of climate and environmental conditions for the recent past to the last 800,000 years. For instance, the compacted snow (firn) in the accumulation zone of the major ice sheets acts as a unique archive of old air, preserving a continuous record of atmospheric composition from the present up to a century back in time (Battle 1996).

Thus, ice cores can be considered as precious and reliable “proxy data”, which are able to report the past climate variability at various time scales. They keep information on the evolution of the atmospheric chemistry composition, as well as of the history of many trace gas species and even volcanism. Moreover, they contribute to establishing a climate linkage from the Northern to the Southern hemisphere; as it has already been demonstrated by the discovery of a strong relationship between greenhouse gases and climate in Antarctica. Particularly, it is possible to recognise a correlation between the climate conditions of Antarctica, which characterized the last 800,000 years, with abrupt and shorter climate changes in Greenland (J. Jouzel 2013).

The archive consists of three parts, which represent three types of records: the first one takes into account the ice itself (with its isotopic composition,

molecular structure, fabrics) while the second type has as a point of departure solid and dissolved impurities trapped inside the ice. Finally, the third record moves by the chemical composition of air bubbles trapped within the ice. The third differs from the other two. In fact, while the impurities measured in an ice sample derive directly from the precipitation event which produced such specific layer of ice, the air bubbles observed inside an ice sample do not have the same age of the ice itself. This difference in the timing is caused by the air bubbles occlusion which is foundable only at the depth of the firn-ice transition, typically somewhere between 50 and 100 m (at summit the close-off is at 70 m (Schwander et al. 1993). Above the mentioned transition, the air is free to move and can be exchanged through many interconnected pores till reaching the atmosphere, at the snow surface (Schwander et al. 1993).

A measurement of the air's mixing ratio from ice cores or firn represents not exactly the atmospheric composition at a specific time. The composition is the result of the combination of diffusive-convective mixing processes of the air presents in the firn layer with the gradual occlusion of the bubbles through the close-off area. Therefore, a measurement represents a quite broad age distribution, with a standard deviation of about seven years. The age distribution has been determined by measuring the firn air combined with diffusion models. The age distribution as well as the age difference to the surrounding ice differs from site to site depending on the climatic conditions i.e. temperature and accumulation rate. For the site investigated here (summit, central Greenland) the current climatic conditions result in a close-off depth of approximately 70-m below the surface, which corresponds to 210 years (Schwander et al. 1993). Knowing such age difference is fundamental in order to understand and to reconstruct the evolution of the atmosphere composition.

The potential of past atmospheric air trapped into the ice has been strongly exploited in the 1989, with the Eurocore project. Firn air has been sampled and analyzed over the whole column height for a vast number of gases (Schwander et al. 1993). Once it is trapped the air represents approximately 10% of the entire volume of ice, consequently it has always been quite difficult to extract

and to measure it. Traditionally methods and techniques relied on Gas Chromatography (GC) for the atmospheric methane measurements and they have been improved over time till reaching the configuration of actual spectrometers, which are able to provide very accurate measurements even with very small concentrations (parts per billion).

The Picarro G1301 analyzer represents an innovative and powerful technology because it allows high stability and excellent detection sensitivity thanks to its cavity ring down spectroscopy features. Furthermore, it is able to extract the entrapped air bubbles directly from the ice core samples, strongly reducing the time process of the analysis and bearing very accurate quantification of small methane concentrations. Regarding the advantages and the features of the different techniques a specific paragraph about methane measurements has been developed later (*paragraph 2.3*).

The aim of this thesis-work is to employ the Picarro G1301 analyzer to measure the methane mixing ratio in air bubbles. The whole set up consists of the instrument itself and of an extraction line where a small section of the ice core (about 40-50 g) is melted within a glass vessel. The trapped air is extracted and then transferred to the analyzer itself to be measured. In order to validate the method a comparison was made with the already existing measurements provided by Thomas Blunier, my supervisor, in 1993 (Blunier et al. 1993), on the same samples (from the same ice core) but analyzed with gas chromatography.

Within this paper terms as “concentrations” and “mixing ratios” are used synonymous and are always referred to the number of molecules of the target gas divided by the total number of all molecules present in the dry air mixture.

2. Background

No climate archive other than ice sheets or glaciers records directly the composition of the past atmosphere. Therefore, the analysis of the air bubbles trapped in polar ice sheets or alternatively in some of the tropical glaciers (such as in South America, China and on the Tibetan mountains) represent the unique reliable mean for us to investigate methane past mixing ratios (T. Blunier, 1993).

Past atmospheric air is trapped within ice through the firnification process, in which snow gradually settled and compacted until transformed into ice. (C. Stowasser 2013). The first attempts to extract these samples of past atmospheric air from ice date back to 1950s for carbon dioxide mixing ratios (Coachman, Hemmingsen, and Scholander 1956).

2.1 Methane studies and extraction techniques

Methane in the Earth's atmosphere was discovered by Migeotte (1948), who recognised its infrared absorption bands (4-100 micron) in the solar spectrum. These early measurements shown an average mixing ratio of about 2 ppmv, (i.e. 2000 ppbv) with a homogeneous distribution throughout the atmosphere (FINK et al., 1965).

In 1973, Ehhalt and Heidt exploiting gas chromatography, measured an average of methane in the troposphere of about 1.41 ppm and 1.3 ppmv for the northern and southern hemisphere respectively, i.e. a total amount of $4 \cdot 10^{15}$ g of methane in the atmosphere (Schmidt 1978).

Anyway, systematic and global observations of the methane mixing ratio have been conducted continuously since 1978, showing an average increase in the atmospheric methane of 0.8% up to 1% per year (Blake and Rowland, 1988), *Figure 2.1*. This rise is quite clearly linked to the increasing of human populations and consequently of human activities since the Industrial revolution, in the middle seventies of the XX century. Such a huge rate of increase has been

caused by more agriculture, more fossil fuel production, more waste which also have meant -more methane emissions. According to IPCC, 2014 the annual anthropogenic CH₄ emissions reached about 8 gigaton of CO₂ equivalent. Therefore in order to investigate the future trend of atmospheric methane, it is paramount to exploit its past variations and the natural feedbacks of the greenhouse warming on the CH₄ cycle (Blunier et al. 1993).

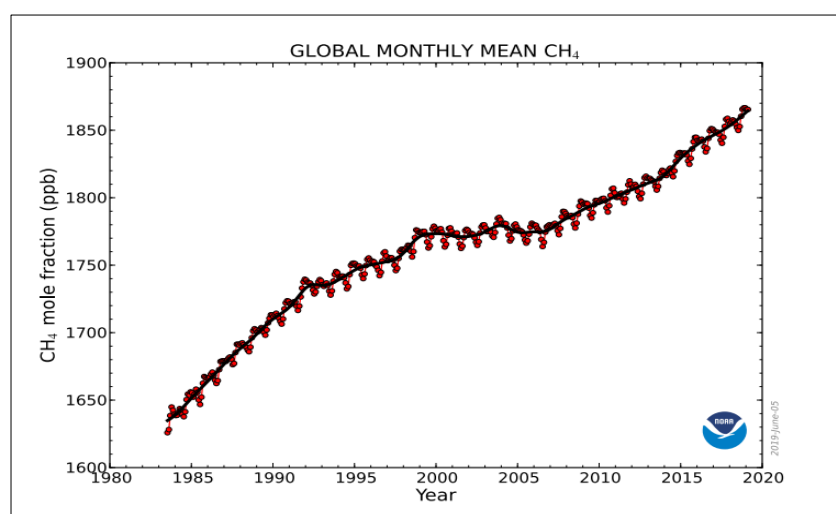


Figure 2. 1 The graph shows globally-averaged, monthly mean atmospheric methane abundance determined from marine surface sites. Particularly it represents the full NOAA times-series starting in 1983. https://www.esrl.noaa.gov/gmd/ccgg/trends_ch4/

According to this curve, it is clearly evident the huge increasing trend which will reach the value of about 1850 ppb in the 2020, against the 1600 ppb or so of the 1980s.

Since the 1950s many researchers have investigated in this topic, developing a variety of techniques to extract the air bubbles from individual ice core samples and to measure the mixing ratio of greenhouse gases inside them (discrete or continuous method). In particular the first analysis of the methane concentrations from ice cores dates back to 1973 by *Robbins et al.* They melted ice samples from Greenland and Antarctica and determined the methane and the carbon monoxide values using gas chromatography. At that time the record

showed low values of atmospheric methane (560 +/- 100 ppb) that mistakenly they attributed to in-situ oxidation of methane into carbon monoxide. Nevertheless some years later *Rasmussen et al.* (1982) demonstrated that those values represented preindustrial atmospheric methane concentrations.

Regarding the technical procedures to extract the air bubbles and to separate them from the ice matrix, there are three main extraction methods that have been utilized for the greenhouse gas species over the past years: the wet extraction, the dry extraction and the sublimation extraction.

➤ **Wet extraction**

The ice core sample is firstly melted within a sealed and evacuated extraction vessel. Then the sample is slowly re-frozen from the bottom of the container, in order to expel the dissolved gases. The containers are usually made of glass, but stainless steel is also used (Sower T. et al. 1997). This sequence of melting and refreezing process forces the expulsion of most of the dissolved air from the sample. After refreezing, the extracted gas is expanded in an extraction line and thus it is injected in the analytical instrument.

➤ **Dry extraction**

During a dry extraction, the trapped gases are liberated without melting ice. The ice core sample is placed into a stainless steel extraction vessel (temperature close to -25°C and pressure lower than 1 mbar) where it is mechanically milled and grated into small pieces to release the occluded air particles. The released air is then flushed into the Gas Chromatography. Although some issues connected with the wet technique can be neglected here, such as the solubility or the water vapour effect, this method still brings several problems: for instance the methane contamination caused from stainless steel surface by metal-metal friction (Fuchs, A., Schwander, J., and Stauffer 1993).

➤ **Sublimation extraction**

This technique is typically employed for gas measurements to separate big amounts of air from ice. Here the ice within a glass extraction vessel is struck and heated by infrared rays down to a temperature just below the melting point. Then the water vapor and the extracted air is cryogenically removed from the vessel through cold traps.

The main difference between these three extraction methods is the extraction efficiency: it is higher than 99% for the wet and the sublimation techniques, which are able to completely free both the occluded air in the bubbles and the dissolved air in the ice matrix; while it is generally below 80% for the dry extraction which does not liberate air from all trapped bubbles and most likely any air from the matrix (Sower T. et al. 1997).

Both the wet and the dry extraction principles are applicable to methane since it does not show any chemical interactions with water (T. Blunier, 1993).

The method I applied relies on a wet extraction process where the extracted air sample is capture on the extraction line of the set up, particularly in the “sample trap”, while the ice core is melting. The trapped sample is then introduced into the Picarro analyzer to determine the methane concentration.

2.2 Methane as greenhouse gas

Methane (CH₄) is a radiatively and chemically active trace compound of the Earth's atmosphere. Overall, it is considered one of the most powerful greenhouse gases with a life time equal to 12.4 years today. Moreover it is regarded to be the second major anthropogenic climate forcing contributor after the carbon dioxide, characterized by a global warming potential far greater than the one of carbon dioxide (over a 20-year period, one ton of CH₄ has a global

warming potential that is 84 to 87 times greater than CO₂) (Lelieveld, Crutzen, and Dentener 1998).

Under natural conditions methane production mainly depends on the continental biosphere. The main processes leading to CH₄ is the decomposition of organic matter under anoxic conditions and specifically in wetlands. Further important contributors are: the enteric fermentation in ruminants and termites as well as the incomplete combustion of terrestrial biomass and the degassing of natural gas reservoirs such as: coal and gas deposits, volcanoes and hydrates in permafrost. A very small contribute is also represented by the ocean (5-10 Tg/year) with the presence of anoxic layers or hydrate degassing at the sediment-water interface. This natural methane production range between 180-250 Tg per year, depending on the estimates (Ommen 2007). Methane also interacts with the global atmospheric chemistry and climate, through many different feedbacks and chemical reactions. For instance, it is to 80-90% removed from the atmosphere through reaction with the OH-radical in the troposphere: $CH_4 + OH \rightarrow CH_3 + H_2O$. Hence, changes in the oxidizing capacity of the atmosphere affects the lifetime of methane. Changes in the availability of OH may have contributed to a minor degree to the observed changes in the CH₄ mixing ratio.

Methane mixing ratio has dramatically changed over the past centuries, particularly over the recent time when emissions originating from human activities started to become more and more massive with the dawn of the industrial revolution. The atmospheric methane burden almost doubled over the twentieth century caused by an increase in biomass burning, fossil fuels use, production and transport of coal, waste emissions, etc.. Such a big surge has brought methane mixing ratio from a previous background of 700 ppbv up to its present day level (1850 ppbv) only in the last 200 years (Blunier et al. 1993). See Ed Dlugokencky, NOAA/ESRL, www.esrl.noaa.gov/gmd/ccgg/trends_ch4. Its growth rate reached 16 ppb/year during 1978-1987 (Lassey et al. 2010), thereafter it slowed down corresponding to a decade-long approach toward

steady state and finally it rapidly increased till a global average mixing ratio equal to 1745 ppbv in 2007, which lead to a methane total load of 4.85 Tg (1 Tg = 10¹² g) (Ommen 2007).

The tropospheric mixing ratio also varies with latitude and longitude: about 10% of CH₄ is destroyed in the stratosphere where CH₄ concentration decrease rapidly with altitude and another 5% is oxidized in soils by the methanotrophic bacteria (Ommen 2007).

The picture below (*Figure 2.2*) shows the socalled “methane flying carpet” or “rug” which represents the methane mixing ratio as a function (smoothed surface) of latitude and time scale since 2001 from the global sampling network. Particularly, it highlighthes the major role played by the tropospheric mechanism, the reaction with the OH-radical, whose concentration correlates with the amout of daylight in each emisphere.

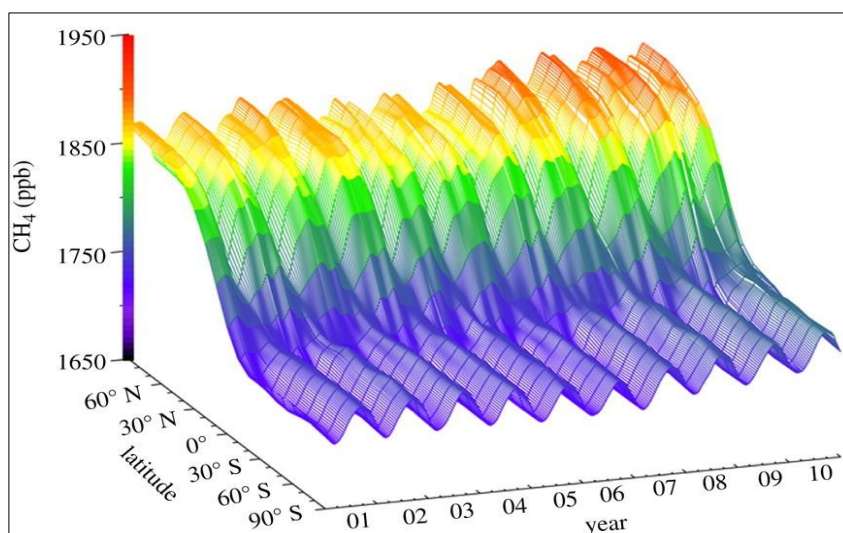


Figure 2. 2 Three dimensional representation of the latitudinal distribution of atmospheric CH₄ in the marine boundary layer, from the US National Oceanic and Atmospheric Administration, Earth System Research Laboratory, Global Monitoring Division (NOAA/ESRL/GMD) programme. Data from the Carbon Cycle cooperative global air sampling network have been used.

2.3 Methane measurements techniques from ice cores

Regarding the measurement techniques, the traditional methods for the definition of the methane mixing ratio from a sample stream typically rely on gas chromatography. Here the air is extracted from individual ice core samples and the methane is separated from the rest of the air components of the sample stream within the column of the Gas Chromatograph (GC), *Figure 2.3*.

Then its composition can be determined e.g. by a Thermal Conductivity Detector (TDC) for oxygen and nitrogen concentrations, or a Flame Ionization Detector (FID) for methane (T. Blunier, 1993). Such kind of measurements of methane mixing ratio from ice cores provided high reproducibility (4-15 ppbv) but they are also very time consuming and destructive kind of processes due to the separation of gas species through the FID.

This prevented consecutive measurements of various gases from a single ice core sample. Furthermore, this method is easy, fast and very efficient (almost 100% of efficiency) (Leuenberg, Bourg, Franchey & Wahlen, 2002), but it needs a dry gas stream, which means that the water must be removed and so that complications to the extraction system, due to the drying process, can occur. Eventually, it cannot

be utilized for all of the gas species; since the process brings vapour transport effects it cannot be applied for highly water-soluble gas species.

The analysis were relied on the GC until 2009, when some new ways to combine melting device, extraction line and gas chromatograph for the analysing process were developed. For instance, the innovative attempt of Schupbach et al. (2009), from the University of Bern, who introduced a combination between a semi-continuous methane detection system (through a

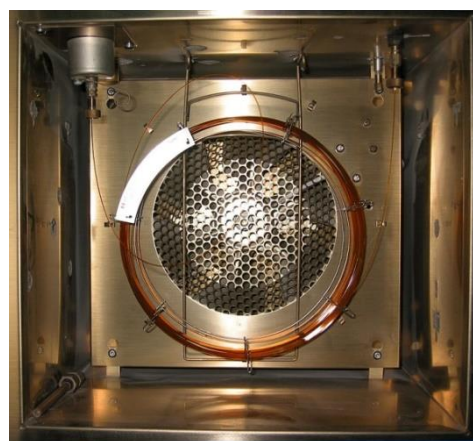


Figure 2. 3 Inner view of a GC in which the capillary column is wound in a spiral around the metal support. In the upper part it is shown the injector (on the left) and the detector (on the right)

GC) and a continuous melting device as in Continuous Flow Analysis (CFA). This new system was all combined in the 2010 campaign at NEEM. It was able to provide faster measurements with high resolution (15 cm).

Over the time then the techniques were refined and nowadays optical spectrometers have become the most utilized analyzer in the fields of atmospheric and environmental sciences, widely exploited for the quantification of greenhouse gas mole fractions of water vapour or other greenhouse gases (C. Stowasser et al. 2014).

The optical technique for these instruments is linked to the specific type of spectrometer selected for the experiment; anyway it is possible to recognize two different measurement conditions with which the optical spectrometers can operate: a **continuous mode** which implies that the sample gas is continuously flushed into the sample cell, and a **discrete mode** which, instead, consists in capturing and collecting the sample before closing the sample cell and then keeping it closed till the end of the experiment. The continuous measurements of methane mixing ratio from ice cores have limitations due to the restricted number of samples (Stowasser et al. 2013). The problem can be solved thanks to discrete methods which also yield high reproducibility and a very important spacial resolution (+/- 3 to +/- 6 ppb; 3 cm at its best).

2.4 Brief history of ice cores drilling

The following section is based on information found in a review of Jean Jouzel (“*A brief history of ice core science over the last 50 yrs*”) and published on the “Climate of Past” magazine in 2013.

Figures 2.4 and 2.5 show the Greenland expeditions sites.

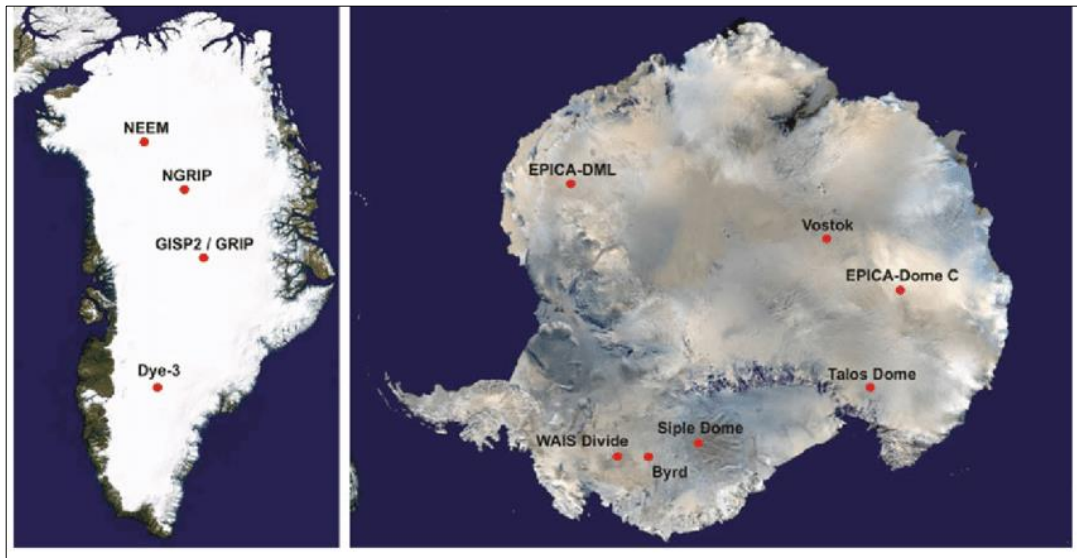


Figure 2. 4 Two different overview of Greenland with the location of the expeditions sites

The first attempt to drill an ice sheet was led by Sorge in 1935 starting from the study of a 15 m deep pit at Station Eismitte, in Greenland. However, the first ice cores, about 100 m deep, were obtained in the early fifties, almost twenty years later, by three separate international projects (Langway, 2008): the Norwegian-British-Swedish Antarctic Expedition on the Queen Maud Land (now Dronning Maud Land) coast (Schytt 1950), the Juneau Ice Field Research Project in Alaska (Report et al., n.d; Miller 1954) and the Expeditions Polaires Francaises in central Greenland (Heuberger 1955). Then, the year 1957-1958 was regarded as the **International Geophysical Year (IGY)** and marked the starting point of ice core studies (Jouzel, 2013). Five countries were particularly interested and active during these early years of deep drilling into polar sheets: USA, the Soviet Union, Denmark, Switzerland and France, often with important collaborations between each other.

Over this period different characters started to emerge: Dansgaard, for example, who was leading the Copenhagen crew, was mostly interested in the isotopic composition of polar snow and its relationship with the temperature at the precipitation site; he was also the first one able to recover continuous isotopic profiles along deep ice cores. Another key role was played by Oeschger, from Bern University, who focused his work on low-level carbon 14-dating; while

Bader and Langway from the US team led the main American drilling expeditions in Greenland. Thanks to these pioneers **Greenland Ice Sheet Project (GISP)** collaboration was born in the early seventies.

Soviet and Russian activities started in 1955 with drilling projects in the Arctic, in non-polar regions, and from the following year in Antarctica too. In 1970 they started the first deep-hole drilling at Vostok within a project also joined by French teams and later by USA. Within this site, they reached a depth of 3623 m (Petit et al. 1999) and they were able to recover the deepest core ever obtained. Eventually, for the first time it has been possible to record a full glacial-interglacial cycle.

French activities on ice cores started in Antarctica in the same period. The first areas reached by the drilling were the coastal regions at proximity of French base Dumont d'Urville (Adelie Land, East Antarctica). Then they involved other teams from Grenoble, Saclay and Orsay in a 905 m deep drilling close to the Dome C. This project allowed them to start new kind of investigations such as measurements of ^{10}Be , the cosmogenic isotope (Yiou et al. 1997), of carbon dioxide (Delmas 1980) of δD and $\delta^{18}\text{O}$ (Jean Jouzel, Merlivat, and Lorius 1982), and of the oxygen 18 of O_2 (Bender 1985).

Australia and Canada represent the last two nations that became interested in drilling ice cores in polar regions in 1970. The Australian team was represented by the National Antarctic Research Expeditions (ANARE). It focused its work on the Indian Ocean sector of East Antarctica and then on the Dome Summit South; they were able to drill very significative ice cores and to reach the bedrock at the beginning of the nineties (Morgan 1997). Finally, Stan Paterson and Roy Koerner were two of the main exponents of the Canadian drilling team. They developed their activities in the Arctic and reached the bedrock around the seventies (Paterson and Koerner 1977).

2.5 Drilling in Greenland

Since I have specifically worked on ice core samples from Eurocore program in Greenland, I briefly describe some of the most important Greenland drilling expeditions of these last thirty years.

The first two big projects took place in two completely distant drilling sites. Both of them were chosen for their accessibility from the two main air bases and for the existing infrastructures (derived from cold war military bases): **Camp Century** in the northwestern part, and **Dye 3** in the South (Figure 4). Both of the sites provided cores

that covered the whole Last Glacial period and highlighted an important succession of abrupt climate changes within the records, yet without any reliable information about the Last Interglacial.

Thus, in order to be able to cover this period the following drilling projects were focused in the centre of Greenland and a bigger international cooperation between US and European teams was agreed in 1987. It was particularly due to Dansgaard, from one side and Wally Broecker, a geochemist and oceanographer from the Columbia University, from the other side, that this project was finally agreed. Dansgaard pledged for the drilling of two cores: one European and the other American. Thus, in the end, the European team chose the highest point for their expedition: **GRIP** (Greenland Ice core Project) while the Americans sites were drilled 28 km farther west: **GISP 2** (Greenland Ice Sheet Project 2) (Jouzel, 2013).

The European site (Eurocore project), which started to be active in 1989 with the involvement of Denmark, France and Switzerland, was dedicated to the recovery of 300 m ice core for the study of the last 1000 years. In 1990 other

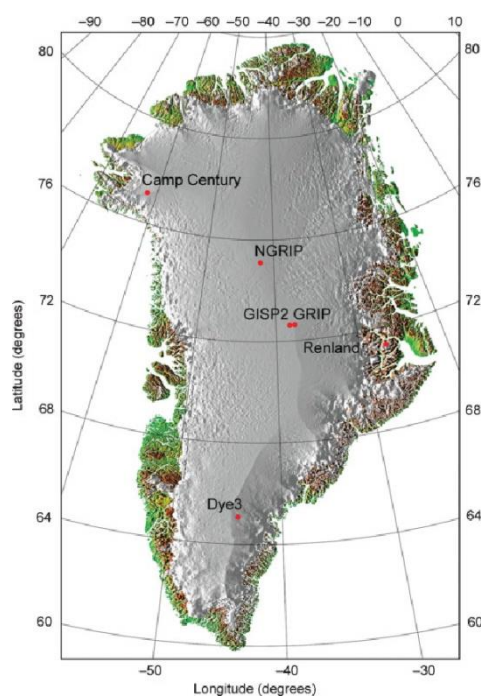


Figure 2. 5 Main Greenland expeditions in red dots

five countries such as Germany, Italy, Iceland, UK and Belgium joined the launch GRIP. After 3 years of drilling, in July 1992, they reached a depth of 3028.8 m (Beng, van Erven, and Wiles 2006). The American team were able to reach the bottom at 3054 m with more difficulties one season later, in July 1993. Anyway for both of the groups of scientists these expeditions were not a complete success: due to characteristic subglacial relief of this area neither of the recovered cores provide reliable climatic information beyond 100.000 years or so (Taylor 1993).

Therefore another attempt was tried, in a flatter zone located 200 km northern of GRIP and in 1995 the North **GRIP** international project (**NGRIP**) was launched, led by Claus Hammer and later Dorthe Dahl- Jensen. In 2003, finally, after years and complications, the drilling ended at a depth of 3085 m. It provided an undisturbed climatic time series of the last 123.000 years, including a relevant portion of the last interglacial period (*North GRIP community, 2004*).

One of the most recent project that ended in 2010, has been developed farther north, between North GRIP and Camp Century, at the **NEEM** site (North greenland **EEM**ian ice drilling). It has involved new countries as China, Korea and Canada and, reaching a depth of 2537 m, it has provided an important record of the last 128.500 years that covers the most of the Eemian (*NEEM Community members, 2013*).

2.6 Eurocore project

In the context of the Eurocore project, as mentioned above, in 1989, a 304 m long ice core was recovered at Summit (72.58°N, 37.64°W; mean annual temperature of about -32°C and mean accumulation rate equal to 209 kg/m²/yr), in Central Greenland, for the atmospheric reconstruction of the last 1000 years. This area also represented the same site of the following Deep drilling GRIP (1993). For the Eurocore project the drilling activities were conducted electromechanically and, opposed to the Deep GRIP application, in dry conditions. The absence of any drilling fluid, together with low temperature,

excludes any potential contamination from drill liquid (Blunier et al. 1993). Age distribution (Δ age) has been determined from firm air measurements on multiple parameters. Air samples were collected from a drill hole in the firm at several depth levels. They were specifically analyzed for ^{85}Kr , CO_2 , CH_4 , CFC's contents and for isotopic composition of nitrogen and oxygen (Schwander et al. 1993). The core was also dated with an accuracy of ± 2 years by combining seasonal variations of δD and $\delta^{18}\text{O}$ with electric conductivity measurements and chemical data. Other timemarkers such as acid layers of volcanic eruptions were exploited for cross-checking. Moreover, based on the density and closed porosity data from the firm core, it has been possible to identify the occlusion depth for the air bubbles. It was mainly between 65 and 80 m corresponding to densities of 790 and 830 kg/m^3 respectively (Schwander et al. 1993).

Eventually, the age difference between the ice and the mean age of the trapped air was calculated about 210 years. Due to the diffusion within the firm, the air bubbles were characterized by an age distribution with a standard deviation of about 7 years (Blunier et al. 1993).

3. Analyzer structure and components

3.1 Cavity Ring-Down Spectroscopy (CRDS)

For the development of my analysis I employed the Picarro Analyzer G1301 (Figures 3.1 and 3.2), which is a **standard Cavity Ringdown Spectrometer (standard CRDS)**.

It is an extremely sensitive detection instrument (able to provide measurements down to ppbv level). This type of

instrument is widely used in atmospheric and environmental sciences, for trace gases (for some species even to pptv level) or isotopes concentrations quantification.

This technique exploits optical absorption spectroscopy of the target gases in order to determine their concentrations.

The Picarro analyzer is an innovative instrument characterized by a high degree of stability and an excellent detection sensitivity that makes it well suited for remote measurement sites. (C. Stowasser et al., 2013).

The G1301, in particular, is designed to measure methane, carbon dioxide and water vapor concentrations.

Such a kind of analyzer relies on the **Cavity Ring Down Spectroscopy (CRDS)**: a technology in which the radiation pulse of a specific wavelength from a laser is introduced into an optical chamber (cavity) through a partially reflecting mirror, one of the three specific mirrors of the cavity. Thanks to the



Figure 3. 1 Picarro analyzer



Figure 3. 11 Picarro G1301 from a laboratory view.

multiple reflections between the mirrors, it re-circulates many times through the sample, creates a very long effective path length and interacts with the sample.

(Figure 3.4)

In this way it is possible to make an idea of the absorption of this light radiation simply by measuring the light quenching when passing through the sample.

3.2 Theoretical background: the optical absorption and the “ring-down” time

The absorption phenomenon occurs only at the specific wavelength in which the transition between two quantum mechanical energy states takes place. This transition energy level is extremely linked to the atomic masses, thus it is different between different isotopes. For this reason each small gas-phase molecule shows a specific and an unique near-infrared absorption spectrum which makes us able to distinguish and recognize one specie to another.

At lower pressure (< 1 Atm) the absorption spectrum consists of a series of well spaced and resolved narrow, standing for characteristic wavenumbers. Since their wavelength is well-known, the concentration of any species can be derived by measuring the strength of this absorption, i.e. the height of a specific absorption peak. In conventional infrared spectrometers, trace gases provide too small absorption to measure, typically limited to the parts per million at best. This sensitivity limitation is avoided through CRDS by using an effective pathlength of many kilometers, which enables gases to be monitored in seconds or less even at parts per billion (some gases at trillion) level.

Therefore in the standard CRDS the mole fraction and the isotopic ratios are calculated from the optical absorbance of the sample (also called *Loss*) and they are obtained in *ppm/cm*, i.e parts per million of loss per centimeter of path length in the sample.

The amount of the *Loss* is derived by another important parameter: the so-called “cavity ring-down time” (τ). It is defined as the necessary time it takes for the

light intensity in the sample cell (high finesse optical cavity) to decay to e^{-1} of its initial value, after light injection into the cavity has been interrupted. It is constantly measured by the photodetector.

A short cavity ring down-time means an high amount of absorbing molecules which also correspondes to a high mole fraction (C Stowasser et al. 2014).

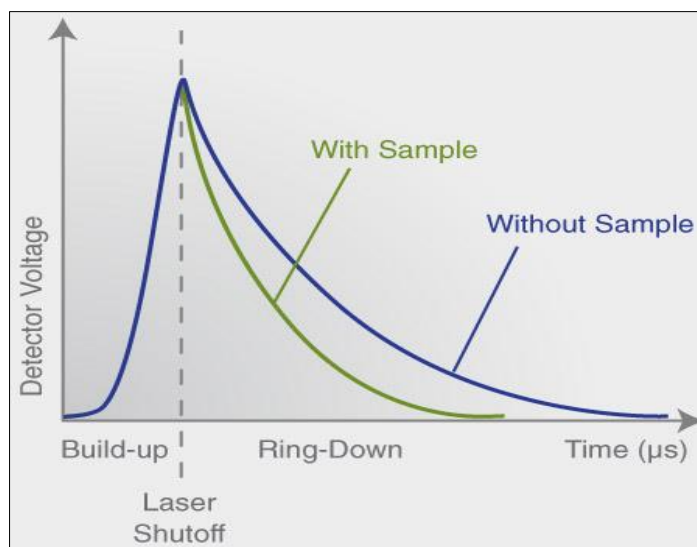


Figure 3. 12 Light intensity decay path in the chamber without sample (blue) or with sample (green)

Initially, without any sample flushed inside, the empty cavity is characterized only by mirrors and lasers: the beam from a single-frequency laser is conveyed into the cavity and reflected by the mirrors. Thus, the photodetector records the light leaking through one of these mirrors and generates a signal that is directly proportional to the light intensity in the cavity. Reached a certain threshold level, the laser turns off and the radiation intensity starts to decay exponentially to zero. In this case the “ring-down time” for the light intensity is uniquely linked to the fact that the mirrors do not have a 100% reflectivity but steady leaking of light intensity takes place.

Once the sample (our gas flow) is introduced into the cavity its presence absorbs the laser light, adding another intensity decay effect and eventually resulting in a shorter “ring-down time”, *Figure 3.3*.

The Picarro instrument automatically calculates and compares the ring down time of the cavity with and without absorption due to the target gas species and it directly converts the number of scans, i.e. the number of spectral scanning, into gas concentrations. This provides accurate, quantitative measurements that account for any intra-cavity loss that may be changing over time, and it enables the discrimination of loss due to absorption from losses due to the cavity mirrors. Moreover, the final concentration data is particularly robust since it is derived from the difference between these ring down times and is therefore independent of laser intensity fluctuations or absolute power.

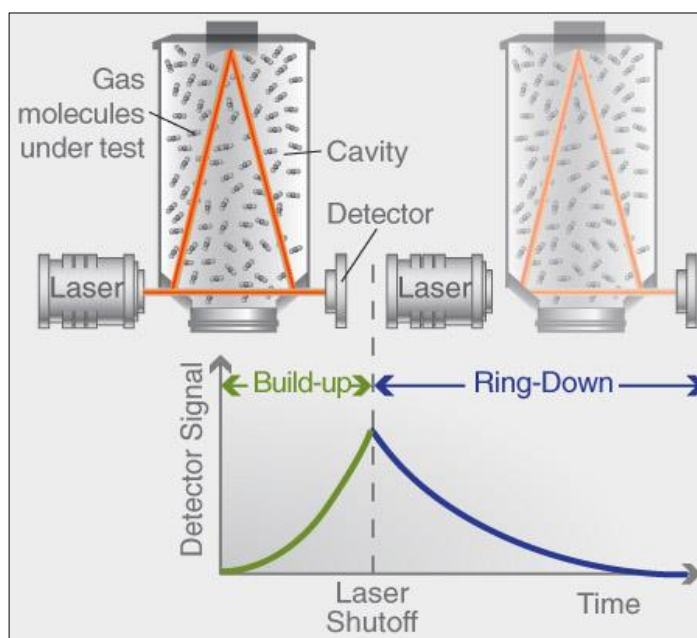


Figure 3. 13 Principle of cavity ring down measurements top left: the beam from a single-frequency laser diode enters the cavity. Top right: the light in the cavity rings down where the ring down time depends on the presence of the absorbing gas. Bottom: The detector signal during the measurements

The temperature and pressure of the cavity, as well as the laser beam wavelength, define the relationship between the light intensity in the cavity and the concentrations of the target gas. For this reason these parameters need to be stabilized and monitored during the experiments. Hence, the analyzer is

designed to be able to control both temperature and pressure: for the first one, it is built by thermally insulated walls that assure a high degree of thermal stability. Regarding the pressure stabilisation, it adjusts the inlet and the outlet valve values by itself, on the base of the sample pressure it records. However, reaching and maintaining steady value for cavity pressure was one of the main challenge of my work with the analyzer.

In order to have an analytical point of view of the physical quantities that I have just described, the Lambert-Beer law provides a formula to calculate the intensity of radiation registered by the detector at a certain wavelength (λ) when passing through the gas sample:

$$I(\lambda) = I_0(\lambda) \exp[-\alpha(T, \lambda)L]$$

Where $I_0(\lambda)$ is the intensity of the incident radiation, α is the absorption coefficient, L is the length of the optical path in the “absorber”, and T is the temperature of the mean.

The absorption coefficient (α) is proportional to the concentration of the gas N , and its characteristic absorption cross section σ :

$$\alpha(T, \lambda) = \sigma(T, \lambda)N$$

Anyway, for the CRDS it is usually exploited the area underneath selected absorption lines of the analyte (or line strength $S(T)$) which is related to the absorption coefficient by

$$\alpha(T, \lambda) = NS(T)g(\lambda-\lambda_0)$$

where $(\lambda-\lambda_0)$ stands for the normalized line shape (Wojtas, 2012).

3.3 The Analyzer description

The Picarro analyzer technically consists in two main working compartments (*Figure 3.5*):

- **DAS: Data Acquisition System.** This contains the spectrometer and the sample chamber. It sends spectroscopic information to the control computer and controls the operations of the system converting spectroscopic data into gas concentration values. Here it is possible to distinguish 2 sub-compartments: the Warm Box, with a temperature around 45.5 °C, that contains the lasers and the Hot Box with the Cavity itself.
- **PVU: Power Vacuum Unit.** This includes a Diaphragm pump to draw the sample, and a computer. Its main function is to convert AC (alternating current) power into DC (direct current) power to drive the analyzer.

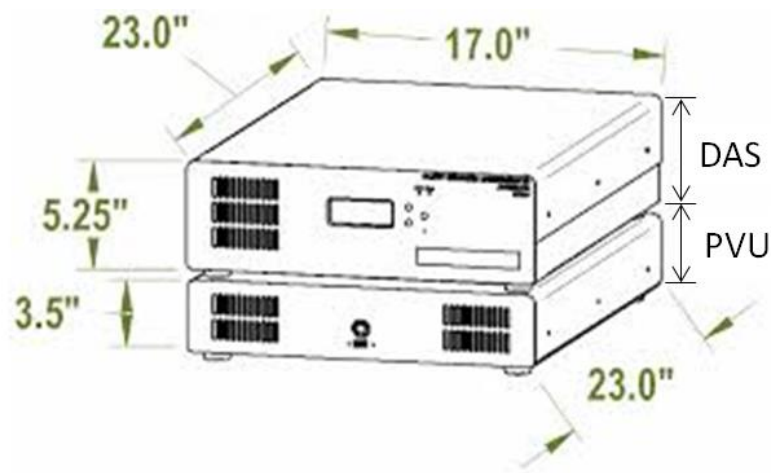


Figure 3. 14 DAS and PVU compartments

Furthermore it is possible to distinguish some other main components which make up a basic cavity ring-down spectrometer: a **high finesse optical cavity** (or sample cell), characterized by three high-reflectivity mirrors, **two lasers**, a **high precision wavelength monitor**, a **photo-detector** and a **computer** (*Figure 3.7*).

The G1301 analyzer is also equipped with an interactive Graphical User Interface (GUI) which allows the operator to interact and to actually work on the instrument. Through the GUI it is possible to start or stop the log files, to change parameters, to regulate the pressure, the inlet or outlet valves; to monitor data and to see the results of the measurements, besides shutting off the system once it is needed. (Figure 3.6)

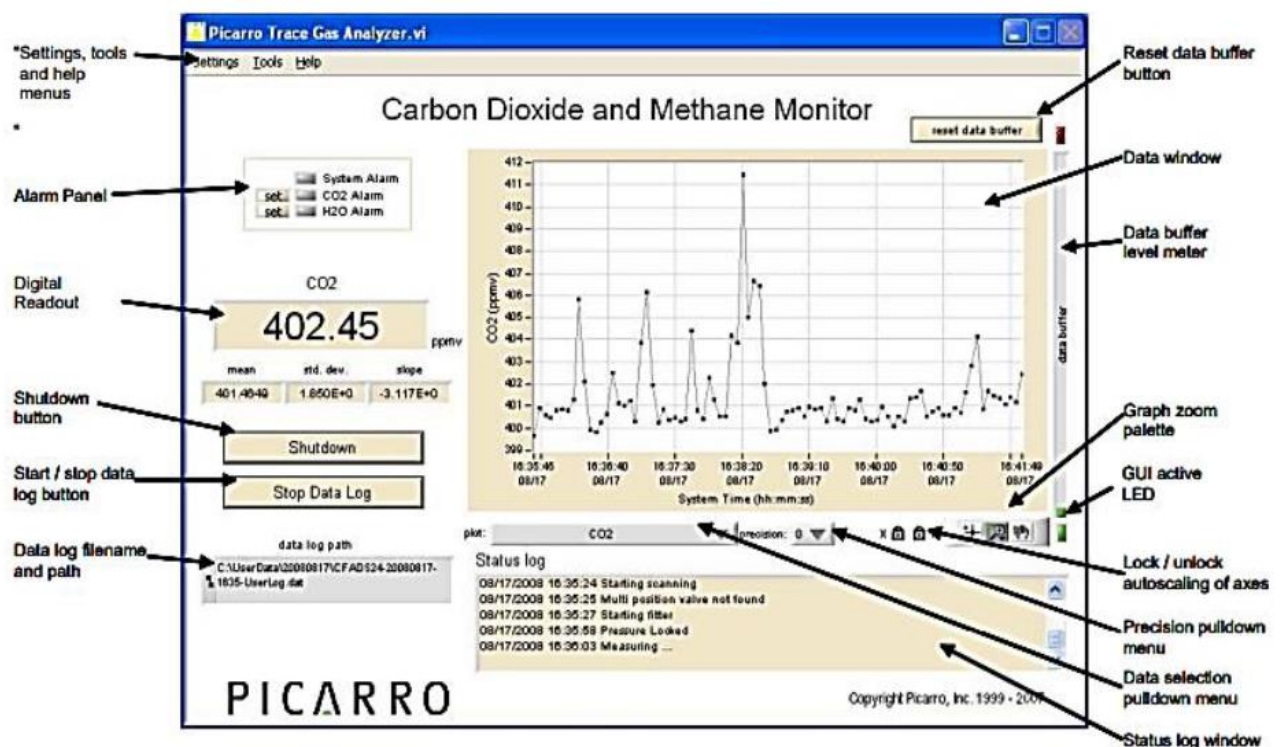


Figure 3. 15 Screen shot of the GUI user interface of the analyzer

The “Data selection pulldown menu” is the most important window because it allows to select which parameter to monitor; for example “methane” option can be chosen making the operator able to see in the “Digital read out” display its measured concentrations over the time. “Status log” shows continuously the status of the instrument; it updates the measurements every 5 seconds and it is very useful to follow and to keep controlled the ongoing measurements. The analyzer is built to be able to save all the data by itself at the drive (CFDSXXXX). These data should hold the record of the last 24 hours-measurements but actually it has been necessary to create a new folder every

day to let the system save the record in different files for different days. These recorded files include: cavity pressure and temperature, DAS pressure and temperature, inlet valve value, outlet valve value, CO₂ concentrations, CH₄ concentrations, water vapor concentrations, flow rate, etc.

The lasers

Regarding the lasers, two **telecom-grade** distributed feedback lasers (DFB) are installed inside the Picarro. One laser is set for the measurement of CO₂ spectral feature at a wavelength of 1603 nm, while the second one measures CH₄ and H₂O spectral features at 1651 nm wavelength. They are able to produce a high resolution absorption spectrum of each specie, from which the constituent fractions of the gas samples are determined (Chen et al. 2010).

The specific features for methane is due to a quartet of transition of the ¹²C¹H₄ molecule which is only partially resolved at the operating temperature (45°C) and pressure (140 Torr) of the instrument. Moreover, for methane measurements the laser tunes over the spectral region between 6,056.96-6.056.25 wave numbers where there are no relevant absorption peaks due to other common atmospheric constituents. Eventually, an ethanol-based optical wavelength meter is mounted to keep centered and to control the laser, with a precision even better of 1×10^{-4} wave numbers. (C Stowasser et al. 2014).

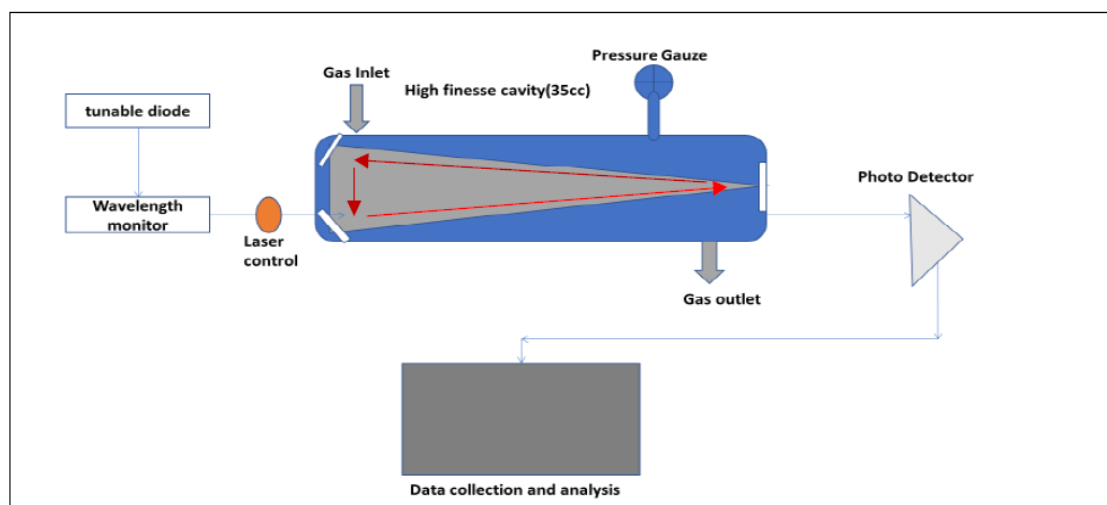


Figure 3. 16 Simple scheme of the complete inner structure of the analyzer

The light for the lasers is selected using an optical switch and it is transported through a polarization maintaining optical fiber till a wave length monitor. Therefore, the analyzer records the loss and the wavelength at each spectral point. The measurements of CO₂, CH₄, and H₂O concentrations are provided every five seconds (0.2 Hz) corresponding to a total of 500 ring down (Physics 2008).

From the practical point of view: the light from a laser is injected into the cavity through one partially reflecting mirror. Once within the cavity the light intensity builds up over time and it is monitored by a second partially reflecting mirror through a photo-detector situated outside the cavity. The “ringdown” measurement is made by rapidly turning off the laser and measuring the light intensity in the cavity as it decays exponentially with the time constant, τ . This drop in the light intensity is mainly linked to the cavity mirrors’ losses and to the absorption- scattering of the sample. After shutting off the laser, most of the light remains trapped within the cavity for a long period of time. This creates a significant path length of tens of kilometers through the sample. Such a path length defines the particular feature of the Picarro analyzer, that is its special high sensivity.

The high-finesse optical cavity



Figure 3. 8 Inner disposition of the component into the DAS



Figure 3. 9 High finesse optical cavity

The sample cell of the analyzer (*Figure 3.8 and 3.9*) is machined from an invar cylinder and as already mentioned it is characterized by three high-reflectivity mirrors (reflectivity > 99,995%) to support a continuous traveling light wave. This provides superior signal to noise compared to a two-mirror cavity that supports a standing wave.

The cavity is quite small with an inner volume of 9,6 ml. The interesting and innovative feature is that the G1301 analyzer can work with a very small amount of sample: in fact the cavity pressure can selectively be set at 140 or at 20 Torr, corresponding to an effective internal volume of 1.8 and 0.25 ml (while commercially available optical spectrometers sample cells volumes typically range from tens milliliters to several liters).

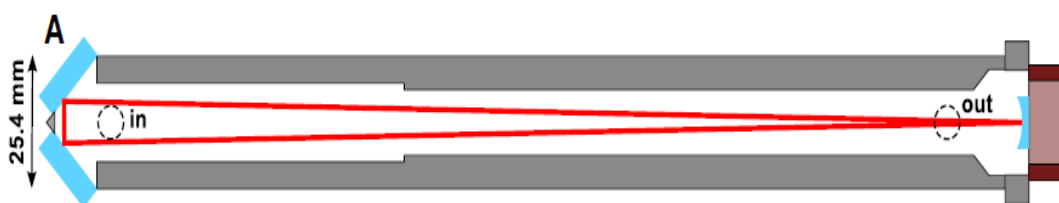


Figure 3. 17 Shows a cross-section through the standard sample cell with the gas inlet (in) and outlet (out) represented as black dashed circles

The red line that creates a triangular shape (*Figure 14*) represents the beam path. The beam travels between three high-reflectivity mirrors (in blue). The two plane mirrors are located on the gas inlet side of the sample cell. One concave mirror is located in an invar ring which is attached to the gas outlet side of the cavity body. This invar ring (in darker red) is a piezoelectric resistor that controls the position of the concave mirror, adjusting it over a small range (1-2 microns).

The internal volume of the sample cell including the invar ring is ca. 35 cc (C Stowasser et al. 2014).

Two high-purity gas filters (Wafergard II F Micro InLine Gas Filter, model WG2FT1SS2, entegris Inc., Chaska, MN, USA) remove particulates from the sample gas before it enters the sample cell, to avoid contamination of the high-reflectivity mirrors. A vacuum pump generates a gas flow through the sample cell and in addition two control valves, called **inlet** and **outlet valve** (EPC Proportional Control Valve, model EP-CAXXSSVXAA, Parker Hannifin Cooperation, Cleveland, OH, USA) regulate the sample cell pressure. They are respectively located upstream and downstream of the sample cell.

Table 1. The following table shows in detail some of the specific parameters which characterized the analyzer (https://www.picarro.com/assets/docs/CO2_CH4_flightanalyzer_datasheet.pdf)

Parameter	CO ₂ Specification	CH ₄ Specification	H ₂ O Specification
Precision (1-sigma over 30 secs, vibration @ 20 Hz, 1g):	< 200 ppbv	< 1.5 ppbv	< 100 ppmv
Drift at STP (Peak to peak of 300 second average):	< 200 ppbv over 30 hours	< 1.5 ppbv over 30 hours	< 100 ppmv \pm 5% of reading
Drift with Changing Temp (30 second peak to peak over 3 hrs; 15°C/hr within range 10-35°C):	≤ 7.5 ppbv/°C	≤ 0.05 ppbv/°C	N/A
Drift with Changing Pressure (30 sec peak to peak over 3 hrs; <1.4 Torr/sec in range 250 – 760 Torr):	≤ 700 ppbv	≤ 7.5 ppbv	N/A
Operating Range	300 ppm to 700 ppm	300 ppb to 2,600 ppb	0 – 2.5%
Measurement Interval (Mode 1)	< 2 seconds	< 2 seconds	< 1 minute
Measurement Interval (Mode 2)	< 5 seconds	< 5 seconds	< 5 seconds
Rise/Fall time (10-90%/90-10%)	< 2.0 seconds	< 2.0 seconds	N/A

Parameter	Value
Inlet gas temperature	10 °C to 35°C
Inlet gas pressure	250 – 1000 Torr
Inlet gas flow rate	0.35 to 0.45 L / min
Variation in Gas Flow	20% peak to peak (From 250 Torr to 1000 Torr)
Gas type	oil free ambient air, non-condensing

Parameter	Value
Ambient Temperature Range	+ 10 to + 35°C
Maximum Rate of Change in Ambient Temperature	15°C/hr
Relative humidity	0 % to 100%, non condensing
Power dissipation	< 370 Watts, steady state
Warm-up time from off	< 1 hour @ + 15°C
Maximum Aircraft Altitude	Altitude @ 250 Torr
Maximum Rate of Change in Altitude	1000 meters per minute

4. Experimental set up and calibration tests

The main component of the experimental set up, i.e. the Picarro analyzer, has been already discussed in the previous paragraphs; therefore this chapter will be focused on the step-wise development of a complete experimental set up for discrete measurements of methane mixing ratios. In particular it will consider the extraction line and its check through different kind of tests.

Noteworthy is the fact that even in this case, where an innovative technique is employed, a dry gas flow, which previously represented disadvantages for GC, is needed for the analysis. The reason is that the Picarro analyser can measure on slightly wet air sample (especially since it also measures water content), but because a wet extraction is exploited, the water vapor obtained is much more than the acceptable. Therefore, the water vapor trap on the extraction line (which is explained in detail below), represents the paramount extraction point, able to capture the water and to keep it around 0.05% by volume before the introduction. Without the water vapor trap, the moisture would dilute the sample flow bringing other effects, such as different methane concentrations due to different humidity content.

The first step was focused on preliminary tests and calibration experiments which led to modification of the different components of the early set up and extraction line in order to identify an optimal set up for the experiments with the real ice core samples. Whereas the second part of this chapter, discuss about the calibration procedure.



Figure 4. 1 Laboratory station: Picarro analyzer on the left and the extraction line on the background

4.1 Experimental set up and component description

The following section describes the basic components of the extraction line which have been employed during the preliminar and calibration tests with a specific focus on the last configuration of the system that it has actually been utilized for the experiments with the real samples.

Table 2 : Name of components employed in the experimental set up

Instrument class	Manufacturer	Quantity
Valves (SS-4H) 1/4-inch (0,635 cm)	Swagelok	5
Valves (SS-2H) 1/16-inch (0,159 cm)	Swagelok	2
3-way valves (SS-4H) 1/4-inch (0,635 cm)	Swagelok	2
3-way valves (SS-4H) 1/16-inch	Swagelok	2
Pump (HiCube Eco 80)	Pfeiffer	1
Pump (Diaphragm)	KNF	1
Pressure Gauge	Pfeiffer	2
Flow censor	Henrywell	1
Flow controller (max 35 cc/min)	Porter	3
Pressure regulator (0-400 mBar)	Bronk Horst	1
Analyzer (CRDS)	Picarro	2
Glass vessel (180 ml)		3

The extraction line was mainly characterized by three fundamental parts: the *sample extraction line* (volume of 6.13 cc), the *water vapor trap* (volume of 25.32 cc) and the *sample trap* (volume of 18.75).

The whole structure is made by a system of tubes and valves; the Swagelok SS-4H bellow valves are denoted by numbers 0, 1, 2, 3 and 4 as shown by *Figures 4.1 and 4.3*. The sample extraction point is comprised between valves 1 and 2, then between 2 and 3 there is the water vapor trap and eventually the sample trap between 3 and 4. There was also another important valve, the number 5, which was situated on the Picarro itself, just before the entrance to the cavity. The latter was a three-way valve and it allowed to connect the Standard line, the Picarro and the extraction line together. During these early experiments it has been necessary to switch it for a suspicious production of methane due to metal-metal rubbing during the opening or the closing of the valve.¹ The water vapor trap is a piece of stainless steel tube of 32 cm length and quarter inch of internal diameter, made with a U shape and filled with glass beads. Their surface area increased with lower temperature; such feature is exploited in order to capture and remove the excess of water vapor from the sample while it is travelling through the extraction line, towards the sample trap. A Swagelok filter protection (10 microns) is placed at both ends of the tube, besides two U-torr (Swagelok) connections for the installation to the set-up. The sample trap is the place within the extraction line in which the air sample is collected. Its volume is about 18.75 cc and it is made up with a quarter inch tube of about 8 cm length. Specific amount (45 mg) of HayeSep D (Product n° 10282, Supelco, Sigma-Aldrich Inc/Dk, mesh; 60-80 surface area; 582 m²/g; max temperature supported: 290°C) is kept inside the tube, in order to capture the specific sample

¹ Such a issue was already investigated during another master thesis project before mine, which exploited a similar set up. It highlighted that it is something linked to the SS-4H valves (stainless steel): the carbon species near the surface of SS are supposed to pick up oxide layer and not be able to across this. When the friction occurs between two metal body, such oxide layer is temporary destroyed causing methane production. It actually also depends on the strength of the operator during the opening/closing of the valves, and after some tests what I have experienced was that it did not affect my measurements except for valve number 5 that therefore was switched.

volume that I want to analyze (see paragraph 4.3.2 *Memory effect*, for more details about sample trap properties).

In the last experiments, before starting to work with real samples a glass vessel of 180 ml volume was attached to the system by a U-torr connection, under the sample extraction line (between valves 1 and 2).

The extraction line is connected to the Picarro analyzer through a 1/16 inch diameter tube with a length of about 40 cm. During the first calibration tests different sizes of capillaries (with thinner inner diameter: 0.150, 0.70 and 0.50 mm)



Figure 4. 2 Hi-cube turbo pump

have also been employed, instead of tubes, to make this connection. They would have represented a stronger restriction on the flow and they would have allowed me to better control it. However, since the length of the capillary must be calculated before its application, in order to get the needed flow, ultimately its connection to the Picarro became too complicated, due to the short length and it was switched with a 1/16 inch tube.

Eventually, there was a turbo pump (Hi-cube 80 Eco, *Figure 4.2*) connected to the extraction line. Such a kind of pump was always employed during the evacuation of the set up before any introduction of the flow for the experiments. It usually combined a Diaphragm pump with a Rotary pump to reach a better vacuum condition, both for the extraction line and the cavity itself. Through the diaphragm pump the set up could reach about 2.6 mBar, whereas with the rotary pump even 10^{-6} mBar. The digital screen on the extraction line (pressure gauge) was useful to monitor the pressure during the evacuation of the whole set up and most of all to handle the introduction of the sample air into the cavity; it also allowed to switch on-off the two pumps.

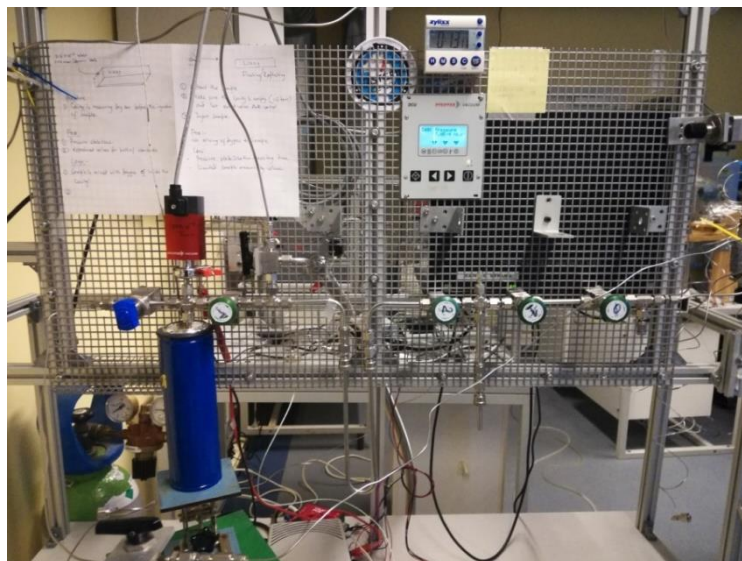


Figure 4. 3 Initial sequence of valves along the extraction line. In the upper central part:the digital screen of the Pressure gauge.

The latest configuration of the extraction line consisted in the basic extraction line structure (described above) with an additional line (on the left) connected before valve 0. It was exploited for the standards (see *Figure 4. 4* below) and it comprised two new valves: valve P, linked to the Turbo pump for a faster evacuation of that section and valve S which regulated the standards flow.



Figure 4. 4 The latest configuration of the extraction line with additional valves: S and P

4.2 Development of the experiments on the set up

Before starting to work on real samples, it has been necessary to verify that the Picarro analyzer provided reliable measurements of concentrations, and that it was able to work in a steady mode even at low pressure and low flow: the necessary conditions for this study.

For all the early experiments, before the real samples air, it has been employed the *EGRIP 2017 bottle* (compressed air), which contains Greenland air from the East GRIP campaign in 2017.

The spectroscopy of the analyzer is calibrated for two different cavity pressures: 140 and 20 Torr. Most, experiments have been reproduced for both these conditions. Most of the issues has been encountered working with low value of the cavity pressure (20 Torr) or with low flow (very close to zero): the most complicated settings for the analyzer to handle with. More details about the kind of issues will be explained in the *4.3 paragraph*.

Table 3 Compressed air composition for CH₄ and CO₂

Pressure (Torr)	Methane (ppm)	Carbon Dioxide (ppm)
20	2,13	197
140	1,98	376

4.2.1 Re-calibration of the analyser flow meter

In order to confirm that the flow meter installed inside the Picarro analyzer was properly calibrated and that it correctly measured the flow, the system has been connected to an external flow meter and the flow has been measured by both of them. Such an external flow meter was already calibrated and accurate, therefore in case of differences between the two measurements, the one installed on the Picarro needed to be re-calibrated directly through the software (Python).

During this test the cavity pressure was set equal to 140 Torr as the measurements were precise and the flow generally is higher at these pressure conditions, so that the eventual differences on the flow would have been more evident. Hence, some measurements only focused on the flow have been done. Differences have been observed in the two flow measurements, thus the Picarro flow meter had to be re-calibrated. The re-calibration relied on the external flow meter settings. In particular the formula on the Python script, which contains the settings for the Picarro flow meter, has been modified by entering the values from the trend line of the external flow meter ($x = 0,02957$, $q = - 241,82$), instead of the original values (*Figure 4.5*).

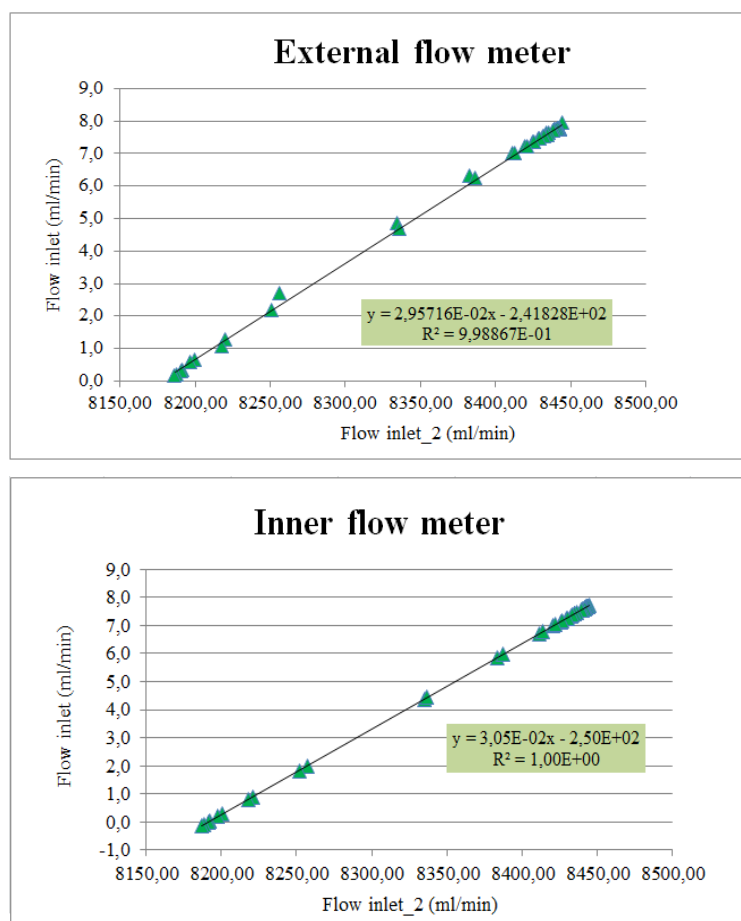


Figure 4. 5 The flow inlet_2 represents the actual signal from the flow mete, i.e. the voltage needed by the flowmeter and it is from that value the flow is calculated. This is converted into a flow, by fitting the voltage reading with the flow readings from a second flow meter. In fact, plotting flow inlet (ml/min) versus the flow inlet_2 is a perfect fit, as they are related by a linear fit by design. The upper graph shows the measurements taken by the external flowmeter. It provides the equation for the recalibration of the analyzer flow meter (which measurements are shown in the lower graph). The inner flowmeter is not from the Picarro manufactory but it is a Honeywell.

4.2.2 Preliminary experiments procedure

The early experiments simply consisted in the introduction of the test sample: *compressed air*; initially in continuous flow in order to allow the concentrations to stabilize and see the first measurements (both at 140 Torr and 20 Torr of cavity pressure); subsequently with limited sample size (at 20 Torr), i.e. with a specific volume of sample which was trapped between valves 0 and 2 or 1 and 2 (not within the sample trap because the only purpose was to try the procedure) and eventually introduced through the system.

Once trapped, the introduction of the sample air can be developed in two ways:

- **Dynamic method:** the cavity of the Picarro is evacuated by an external vacuum. This is easily commanded through the “sample handling parameter” on the computer controller, changing the inlet and outlet values.
- **Static method:** a dry gas stream is flushed through the cavity. Then the introduction of the sample takes place without any previous evacuation of the system.

The dynamic method has always been employed in all the experiments of this project. The early experiment in discrete mode were developed trapping the sample between valve 2 and 1.

Discrete experiments procedure:

- Starting point: continuous flow from the compressed air bottle; all valves open (except the one on the Picarro, valve 5, that initially was turned to the laboratory air).
- To trap the sample: first of all close valve 4 and then number 0 (to have a constant gas volume inside).

- Close valve 2 in order to have a volume between 2 and 1; open the Hicube pump (with Rotary pump on) in order to reach the lowest pressure possible, i.e. to have the best evacuation.
- When a pressure equal at least to 1 mBar was reached, close the pump; the pressure should have remained equal to 1 mbar.
- Open valve 2 to let the sample enter the trap. Once it reached the pressure of interest (which was around 190 – 240 mBar), note the value and close valve 3.
- Once closed valve 3, it was possible to turn valve 5 to the sample air and to wait at least 5 minutes to let the instrument stabilize.
- Open valve 4 and let the sample flow into the Picarro.

4.3 Challenges in developing the experimental set up

From the preliminary tests and experiments it has been possible to identify four main influential factors which have represented issues for the set up and which had to be monitored, and eventually fixed, in order to get reliable results. These are:

- **Presence of leaks**
- **Memory effect of the sample trap**
- **Cavity pressure**
- **Flow rate**

4.3.1 Presence of leaks

The most common problem linked to this kind of experimental system, has been the presence of leaks, particularly when the analyzer is set to the lowest cavity pressure (20 Torr).

Most of the time it has been caused by screws or connections not tightened enough on the extraction line.

The process of investigating the leaks has been the ones that actually has taken most of the time before starting with real sample experiments. From the practical point of view it is almost impossible to reach a completely tightened system condition, but it is necessary to get an environment as closed as possible in order to prevent any kind of contamination.

For leaks investigation and detection many different methods have been employed; most of these have been applied with cavity pressure set at 20 Torr to have clearer and immediate responses.

The evacuation of the set up has always been very important to prevent influences from residual air of previous flows and to have the best vacuum condition before starting new measurements. The best way to evacuate the system was exploiting both the turbo and the rotary pump for the extraction line, specifically for the section between valve 0 and 4; while for the rest of the set up, between valve 5 till the inner volume of the analyzer, the evacuation was obtained through the Picarro pump (only when a cavity evacuation was necessary). During these measurements the lowest pressure reached on the extraction line, as it will be explained later talking about the monitoring of the Pressure (see *Leak detection methods*), relied on the evacuation time and ranged between: $1.0\text{E-}3$ and $7.7\text{E-}4$ mBar. The minimum value reached for the cavity pressure was: 3.68 Torr.

Leak detection methods:

- ***Flushing CO₂***: One of the easiest and the most direct test was to employ an external gas flow (in my case one between CH₄ or CO₂ flow made sense, since the Picarro G1301 is able to measure only these two gas spieces, besides water), carried from a gas bottle within a tube, and to blow it on each valve or connection of the set up. Simultaneously, the Picarro was measuring the compressed air (that is my test sample) in continuous flow. If one of those connections or screws was not tightened enough or was damaged, it would has resulted, in fews seconds, in a big

jump in the concentrations values on the GUI screen, directly caused by the contamination from this flushed gas flow. For this kind of test a pure CO₂ gas bottle was employed since it was recommended to keep the CH₄ bottle out of the lab, for safety reasons.

- **Flow experiments:** A second method to detect leaks has been to simply monitor the concentrations trend in relation with the flow; changing the inlet, the flow changed (as I have already mentioned) while the concentrations should have remained stable in a “leak tight” system. A continuous growth of the concentrations tending to the values of laboratory’s air composition could mean leaks. Furthermore, another attempt has been to repeat different experiments changing the inlet value and to compare the measured flow for the same inlet value between the different experiments. In this case, different values of the recorded flow could have confirmed suspect of leaks.
- **Pressure experiments:** Monitoring the pressure behaviour from the pressure gauge (Pfeiffer) of the extraction line has been also a way to investigate leaks. After a complete evacuation of the whole set up, in order to get the best vacuum possible (lower pressure condition makes the pressure variation more evident in case of leaks), the aim was to see how much and how quickly the pressure on the extraction line would increase. Different attempts, varying the evacuation time (four days, a whole weekend, a whole night, an hour and half an hour), have been tried. Without any leak the pressure should have reached a very low value during the evacuation and it should have increased slowly and gradually once the evacuation stopped. A further consideration was possible thanks to such a kind of test: as the increasing rate in pressure and its minimum reached value were different with different evacuation time for the system (for instance, the best vacuum reached was: 7.7E-4 mBar, after four days’evacuation, against the 1.0E-3 mBar after just a hour of evacuation), a “memory effect” due to the sample trap was suspected (see “memory effect” paragraph below).

- **Helium bottle detection:** this test has been developed connecting a pure Helium bottle (He > 99,999%, H₂O < 3 ppm, O₂ < 2 ppm, CnHm < 0,5 ppm) to the set up and letting it flow through the instrument. Since it did not contain any nitrogen component, its composition would have been in contrast with the lab air where there was a leak. This test was conducted with a bit of overpressure, as that is necessary for the helium to travel out into the lab. Each of the valves and joints was tested employing a Helium Leak Detector (Agilent technology, G3388A) in order to detect the leak.
- **Pure nitrogen bottle:** this gas bottle was characterized by having no carbon dioxide, methane, water components. It simply consisted in pure Nitrogen (99,95%); therefore letting it run through the instrument would have brought the concentrations equal to zero. This test was also combined with CO₂ flushing method, expecting to see a big jump in CO₂ concentrations in case of leak's presence. Important to not let work the analyzer with this pure nitrogen flow for too long, because working with no concentrations could bring some functional issues in the absorption peaks settings.

In this way it has been possible to identify a modest number of leaks, particularly on the extraction line (connections close to valve 5, valve 4), but also in the Picarro itself (screw close to Inlet valve), which have been completely switched or fixed. One last experiment has been tried after this correction: the whole set up, from valve 0 to valve 4, was evacuated and the minimum value reached for the pressure was 6.4E-4 mBar on the Pressure gauge. Furthermore, monitoring (each minute for 30 minutes) the pressure behaviour, once the evacuation was stopped, the pressure was very stable and it increased slowly, confirming that the system has been leak tightened (*Figure 4. 6*).

4.3.2 “Memory effect” of the sample trap

The sample trap (*Figure 4. 6*), as already mentioned above, is the extraction line point where the sample air is collected. It is filled with a specific amount of special material which enable to trap and held the sample before the introduction, with an efficiency that is inverse related to the temperature. The lower is the temperature, the higher is the absorption capacity. Thus, the role represented by this filler material is fundamental for measurements as the ones of my project. On the other hand, it might also represents a source of issues.

In fact, during the preliminar experiments, especially the ones with limited sample size (discrete measurements) for the three standards (see chapter 5 about *Standards calibration*), it has been observed that the measured concentrations for methane were unreasonable high; they were too high also to be explained as leak effect since the values continued to increase, even exceeding the laboratory air content of CH₄;



CO₂ showed the same behaviour. One hypothetical explanation could be that some

Figure 4. 6 Sample trap between valve 3 (on the right) and valve 4 (on the left)

particles most likely remained absorbed within the sample trap and that they were slowly “released” with low flow (especially during limited sample size experiments) over time. A low flow made gas particles more free to recirculate. Consequently, this resulted in higher values of methane and carbon dioxide as the product of trapped particles from previous flows (even with evacuation before each experiment). Such a “memory effect” seemed stronger for carbon dioxide than for methane: the observed increasing in the CO₂ was lighter than the one for CH₄, which also means that CO₂ was held back longer within the sample trap.

A way to solve this issue consisted in putting a sort of heating system under the sample trap, which was made by a high resistance wire wrapped around the sample trap tube and connected to a thermometer (as shown in *Figure 4.7* and *4.8* below).



Figure 4. 7 Sample tramp with the high resistance wire wrapped around the tube



Figure 4. 8 Whole view of the heating system mounted around the sample trap. The blue container helps to keep the heat and accelerate the temperature increasing.

Even in this case different experiments have been developed letting run the gas flow (compressed air) in continuous and changing the temperature of the heating system (from 170°C to 80°C) in order to establish the best temperature value under the sample trap. Eventually, it has been possible to observe that temperatures above 140°C resulted in too high concentrations and also strange peaks in the fit results (not flat or symmetric as they should be), both for methane and carbon dioxide. On the other hand, temperatures kept at 90°C, or lower temperature, were not enough to allow the gas particles, absorbed by the HayeSep D spherules, to be completely released.

Another similar test has been tried with the compressed air, but this time keeping the temperature of the heating system equal to 100°C and modifying the flow from about 1.6347 ml/min (inlet= 16500 digU) to 0.0300 ml/min (inlet=13500). Even here the results confirmed the important role of the heating set to 100°C: methane concentrations stayed almost constant around 2.14, with a very slight increase in the order of 10^{-3} ppm, which is included in the standard deviation of the measure.

Therefore, in order to avoid overheating effects and to assure that the sample trap was as much empty as possible before the following experiment, the heat was kept to 180°C during the evacuation of the set up and then reduced to 100°C few minutes before the introduction of the sample flow. Since it took me some time and experiments before I recognized it, this issue has been fixed almost at the end of the preliminary phase, therefore note that some of the early experiments run with this kind of problem. However, as far as they have been developed in continuous flow, it should not represent a big deal.

4.3.3 Cavity pressure

The cavity ring down measurement technique relies on a very stable pressure. When this is not the case the results are affected. However, the pressure dependence is very linear and can easily be corrected for. In the following I deliberately offset the pressure and determined the correction for CO₂ and CH₄ respectively for an eventual pressure offset. The early break-in tests with compressed air in continuous flow, have also been developed in order to see the concentrations behaviour once the cavity pressure slightly changed. For reliable measurements, the concentrations should not be affected by any effect, especially the one due to the cavity pressure. The concentrations should remain constant.

These experiments were done with a fairly high flow (about 1.40 ml/min; inlet value equal to 15500 dU) in continuous through the system and with an initial cavity pressure set to 20 Torr. Hence, the cavity pressure was changed every 15 minutes to a higher (20.10 , 20.30 , 20.50 , 21.00 , 21.50 , 22.00 Torr) and to a

lower value (19.90 , 19.70 , 19.50 , 19.00 , 18.50 , 18.00 Torr). Eventually, the influence of the cavity pressure was clear: increasing the cavity pressure, the values increased both for CO₂ and CH₄, while decreasing it the values decreased too (*Table 4*). That is why the instrument should always operate at a stable cavity pressure.

Table 4 Cavity pressure with respective flow and concentrations of CO₂, CH₄ and H₂O

Pressure (Torr)	Flow (ml/min)	Carbon dioxide (ppm)	Methane (ppm)	Water (% vol)	Time
22	1,4208	221,829	2,369	0,017	13:25
21,5	1,4241	217,914	2,317	0,018	13:08
21	1,423	214,179	2,266	0,019	12:51
20,5	1,4138	209,748	2,211	0,02	12:34
20,3	1,4147	208,199	2,191	0,023	12:17
20,1	1,4240	206,963	2,172	0,025	12:00
20	1,2494	204,99	2,1549	0,031	11:45
19,9	1,4013	204,604	2,148	0,015	13:42
19,7	1,3823	203,202	2,128	0,014	13:59
19,5	1,3948	201,59	2,109	0,014	14:18
19	1,3062	197,481	2,055	0,013	14:35
18,5	1,3228	193,539	2,003	0,012	14:55
18	1,2853	189,103	1,95	0,011	15:12

The cavity pressure effect was determined plotting in a graph the methane and carbon dioxide measured values, standardized to the measured value at 20 Torr and expressed in percentage, versus the cavity pressure. See *Figure 4. 9* below. Ultimately, the effect was derived from the slope of the respective linear tendencies: it corresponded to 5% (4,86%) for methane and to 4% for carbon dioxide measurements, which means that for each Torr of cavity pressure the concentrations increased or decreased, depending on the pressure variation, of about 5% for methane and 4% for carbon dioxide.

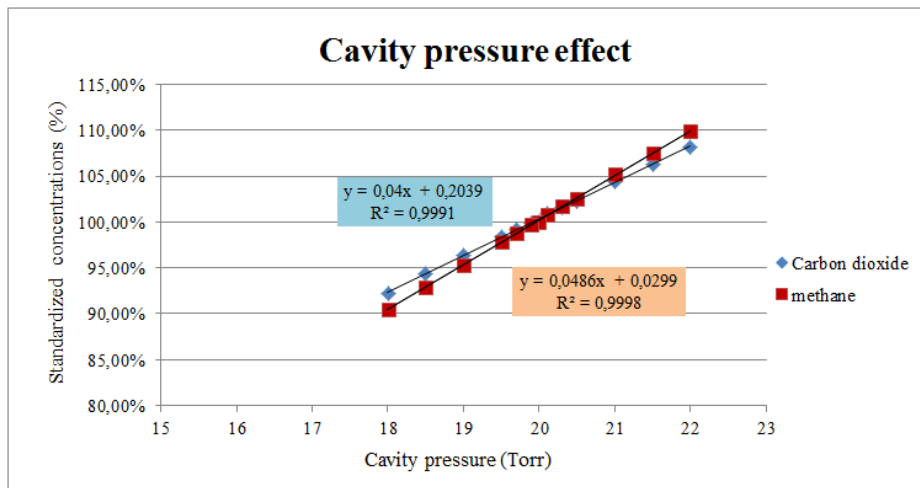


Figure 4. 9 In red squares is shown the methane trend while in blue squares the carbon dioxide trend. Both of them with the respective linear equation.

In order to remove this cavity pressure influence from methane measurements, a correction was determined which relied on the linear tendency from Figure 4. 9:

$$y = 0.0486x + 0.0299$$

$$CH_4 \text{ pressure corrected} = CH_4 \text{ measured} / [1 + 0.0486 * (P_{\text{measured}} - 20)]$$

where **0.0486** is the slope value and **20** stands for 20 Torr, the cavity pressure. Regarding CO₂, the same procedure was followed for the pressure effect correction, considering the respective linear equation and slope:

$$y = 0.04x + 0.2039$$

$$CO_2 \text{ pressure corrected} = CO_2 \text{ measured} / [1 + 0.04 * (P_{\text{measured}} - 20)]$$

4.3.4 Flow rate

The same aim has been pursued with the flow: to see whether the concentrations stayed constant with different flow rates or they changed. For such kind of experiments the procedure consisted in changing the inlet values, thus the flow, every 30 minutes and monitoring the concentrations. Since the memory effect of

the sample trap was already suspected here, a heating system was tested, in order to find the best temperature and avoid it. Three different tests were performed in three days, preceded by a whole night evacuation. Two of them were conducted with the heating set to 90°C and the other with the heating at 100°C. The gas flow from the compressed air bottle run through the set up in continuous and the flow rate was decreased starting from inlet equal to 15,000 down to 10,000 digU. For the data re-elaboration the average of the last 20 minutes' monitoring has been utilized.

Table 5: Measurements from the three tests. It is quite evident the role played by the flow on methane concentrations, whereas it is not the same for carbon dioxide (which explanation is possible recalling the memory effect of the sample trap).

	Inlet (digU)	Average			Standard deviation		
		Carbon dioxide (ppm)	Methane (ppm)	Flow (ml/min)	Carbon dioxide (ppm)	Methane (ppm)	Flow (ml/min)
I test (90°C)	15000	198,4611	2,141684	0,39900	2,87E-01	3,49E-03	3,10E-02
	14900	198,3452	2,142550	0,36040	2,54E-01	3,49E-03	2,99E-02
	14800	198,4310	2,143344	0,37060	1,32E-01	3,62E-03	3,92E-02
	14700	198,6135	2,145130	0,30050	1,85E-01	3,48E-03	3,24E-02
	14600	198,6914	2,146012	0,29220	1,68E-01	3,95E-03	4,63E-02
	14500	198,6472	2,144900	0,29510	1,31E-01	3,69E-03	6,12E-02
	14400	198,6380	2,145304	0,26390	2,98E-01	4,03E-03	5,33E-02
	14300	198,6500	2,146603	0,21380	1,54E-01	3,55E-03	5,14E-02
	14200	198,6726	2,147438	0,16840	1,28E-01	3,35E-03	3,13E-02
	14100	198,7240	2,147629	0,14950	1,17E-01	3,57E-03	3,28E-02
	14000	198,6447	2,148773	0,14790	1,20E-01	3,60E-03	2,20E-02
	13900	198,6952	2,151138	0,11210	1,90E-01	3,58E-03	1,62E-02
	13600	198,7108	2,151359	0,09885	1,25E-01	3,64E-03	1,67E-02
	13500	198,8212	2,152335	0,09570	1,26E-01	3,48E-03	1,83E-02
II test (90°C)	13250	198,3372	2,147842	0,09940	2,41E-01	3,66E-03	2,18E-02
	13000	198,8721	2,149779	0,06990	2,19E-01	3,66E-03	3,83E-02
	12750	198,9785	2,150189	0,05100	2,16E-01	3,75E-03	4,69E-02
III test (100°C)	12500	197,6800	2,151590	0,07903	2,34E-01	3,73E-03	3,68E-02
	12250	197,9506	2,152238	0,07804	2,66E-01	3,81E-03	3,43E-02
	12000	198,1023	2,152162	0,05967	2,74E-01	3,75E-03	4,37E-02
	11500	198,0810	2,151871	0,05345	2,79E-01	4,17E-03	5,39E-02
	11000	198,2317	2,153752	0,02545	3,60E-01	4,72E-03	5,33E-02
	10500	198,2956	2,154079	0,00440	3,48E-01	4,95E-03	4,78E-02
	10250	198,4323	2,155478	-0,01391	4,75E-01	5,56E-03	4,13E-02
10000	198,3724	2,154852	-0,00269	5,51E-01	6,63E-03	4,77E-02	

Even in this case, an effect of the flow rate on the measured concentrations was clear: the lower the flow, the higher the methane concentrations (Table 5). Hence, flow and methane concentrations seemed to be inversely related. When I ran the tests for the lower flows I also observed that the flow meter provided negative values, which stood in stark contrast to the fact that it must had a

positive flow, due to the cavity pressure being maintained with vacuum on the outlet. Trying to add a small positive offset to the measured flow the relationship between methane concentrations and the inverse flow became better. Furthermore, I investigated the offset that lead to the best linear fit, which resulted in an offset of 0.7 ml/min (*Figure 4.10*).

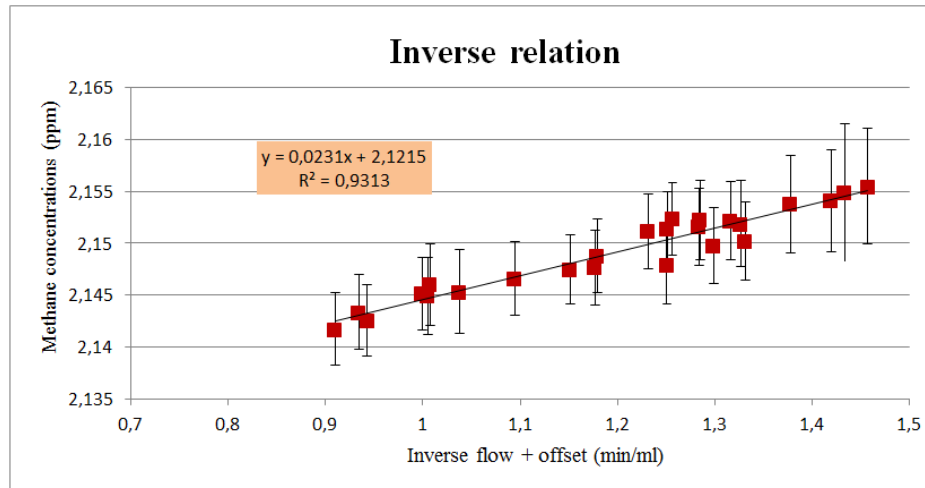


Figure 4.10 Shows the best linear fit between inverse flow + offset and methane concentration. It is represented by the line: $y=0,0231x + 2,1215$

Anyway, even if I have observed such influence trying to correct it, as I had already done for the cavity pressure effect, was not so easy. A similar correction, derived from the graph with methane and inverse flow+offset, has been tried, resulting satisfactory for most of the values, however when it was actually applied to the measurements with low inlet (thus low flow), it still run into issues with methane values way below the expected. Therefore, such an effect could not be treated as a relative or neither absolute, but it is something rather complex. There are too many variables associated with it which I could not determine due to the little time available for my project, but that should represent a crucial point for further investigation. Unfortunately, due to the shortcomings of the flow meter used, giving negative values, it was not possible to implement a satisfying correction for it. It has since further been discovered, from other measurements, conducted during other projects, that actually such effect varied in a non linear manner with CH₄, so implementing the correction

found in this work based on a CH₄ mixing ratio of 2.14 ppm would not be correct for the lower values found in the actual samples.

It has fortunately for this work been assessed that the flow effect will not affect the results, as the flow is rather constant for the averaging period across all the experiments. Furthermore, the calibration gases before the actual samples were measured through the same method, and thus the flow effect should be accounted for by comparison to their true values. In other words, because the flow is very close to being identical for all samples and standards when the average is taken, the flow effect should be more or less equal between the standards and the samples, meaning that since the samples are corrected using the standards, the flow effect is also incorporated into the measured standard value; for this really to hold true, we should compare the average flow for the samples and the standards.

Ultimately, the methane has been cleared of the pressure effect, but not of the flow influence, which would need more investigations and attempts in order to find out all the variables involved. Anyway since it is a constant presence over all the experiments, I can consider it as something included in all the measurements, and therefore that it has not significantly affected the results.

5. Standard calibration

One last fundamental process before starting to work with real samples, was the calibration of the Picarro measurements. In my case, it has occurred through three standards, thus also called “three points” calibration. For such purpose, the experiments were conducted with further two gas bottles, besides the compressed air: Standard 1 and Standard 2, both of them characterized by a well-known composition (see *Table 6*). Initially they have been analysed in continuous flow in order to monitor concentrations and to confirm that the previous correction for the compressed air, was still valid for these two dry air flow. A first calibration was made.

Table 6 Known compositions for standard 1, standard 2 and compressed air. For the compressed air I have considered the values measured at 140 Torr, because at that pressure condition the values were certainly correct.

expected		
	Methane (ppm)	Carbon dioxide (ppm)
Standard 1	0,4	180,000
Standard 2	0,7	280,000
Compressed air	1,98	376,110

The first calibration relied on continuous flow experiments (as up to this point reliable measurements only derived from them) and without any heating system (as the memory effect did not occur with a continuous flow set to about 1.40-1.50 ml/min).

Table 7 measured values for standard 1, standard 2 and compressed air.

measured		
	Methane (ppm)	Carbon dioxide (ppm)
Standard 1	0,437 ± 0,005	93,042 ± 0,714
Standard 2	0,756 ± 0,004	148,477 ± 0,477
Compressed air	2,135 ± 0,004	198,500 ± 0,193

Calibrating methane measurements means that the methane concentrations which will be measured during these calibration experiments, will be corrected on the basis of the relation between the measured (*Table 7*) and the expected values for the three standards.

Thus, the calibration consisted in calculating the ratio between the **CH₄corrected** value and the slope (1.079), from *Figure 5.1*:

$$CH_4calibrated = CH_4corrected / 1.079$$

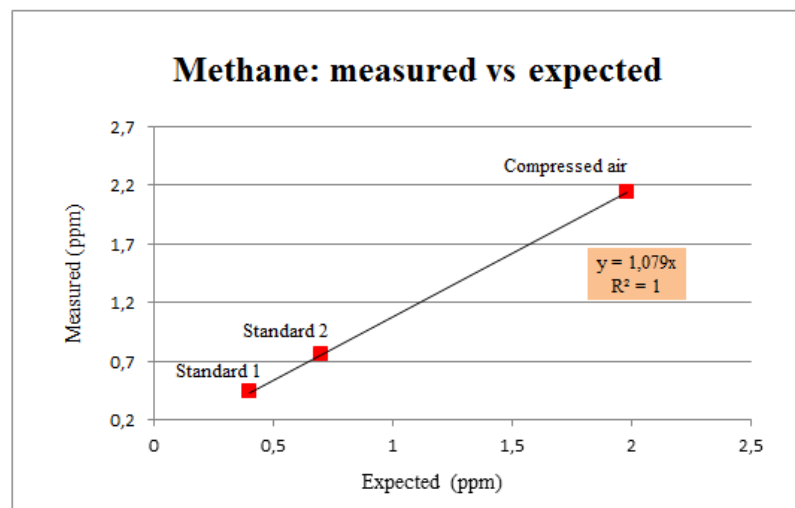


Figure 5. 1 Methane values from continuous flow experiments with the three standards plotting against the respective expected values

The same calibration has been made for CO₂ too. The slope for CO₂ was equal to 0.5272 (*Figure 5. 2*), therefore:

$$CO_2calibrated = CO_2corrected / 0.5272$$

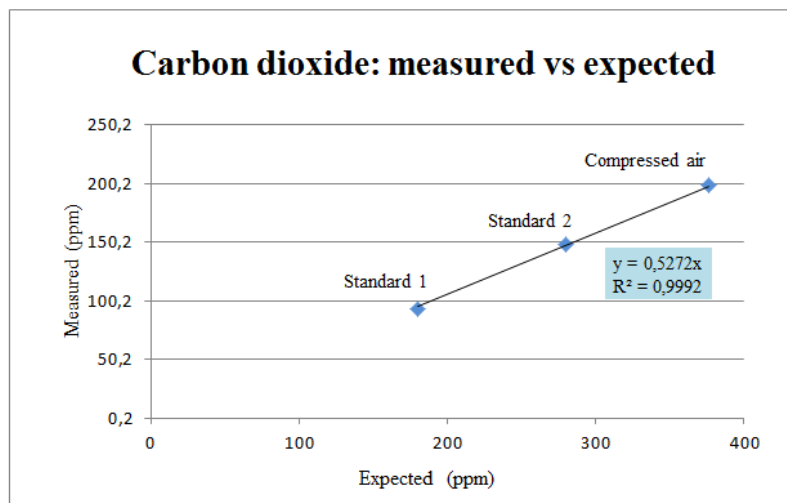


Figure 5. 2 Carbon dioxide values from continuous flow experiments with the three standards plotting against the respective expected values

Then a host of experiments have been developed in discrete mode, i.e. limiting a sample size, in order to verify that the first calibration was reliable for limited volume samples or a new one was required. Eventually, to try an experimental procedure as close as possible to the final one, with real samples.

Different methods have been tried during these last preliminary experiments. Initially, standard 1 and standard 2 have been measured in discrete mode, simply following the limited sample size procedure (see 4.2.2 paragraph). Concentrations showed similar behaviour to the discrete measurements for the compressed air: a first sudden increase in concentrations, followed by a slowdown and a sort of stabilization for CH₄ (even if to a higher value) whereas by an increasing trend for CO₂, without stabilization. The first calibration in this case, with unstable concentrations, might not be completely reliable. Note that it was during such experiments that the issue with memory effect of the sample trap was finally fixed, stabilizing the correct temperature for the heating system (see 4.3.2 paragraph).

Therefore, different sessions of experiments have been developed always with the three standards (analyzed in sequence) in order to get closer to the final protocol and to find the correct calibration. Some of them have been conducted

running the dry gas flow through the set up equipped with a cooling system (liquid nitrogen pot), alternated with the heating system, under the sample trap (*Blank experiments*) as required for real experiments; the others having also a fake ice surface to interact with (an air free ice, AFI), hence connecting the last missing component of the extraction line: the glass vessel, in order to employ a real procedure (*AFI experiments*).

5.1 Calibration experiments

5.1.1 Blank experiments

The three standards were flushed through the system with known and controlled pressure of sample air before the introduction, by using a pressure controller. Since they were dry gases (about 0.01% vol of water vapor), the water vapor trap was not exploited at this stage, thus the liquid nitrogen bath was not applied under it but only under the sample trap. The Picarro operated in dynamic mode.

Procedure:

- Introduce the sample gas (from one of the three standard bottles) in continuous flow and monitor the concentrations. The standards have always been analysed following a sequence: compressed air, standard 2 and standard 1.
- Letting run the flow for at least 20 minutes to allow the stabilization of concentrations around the expected values. Heat under sample trap was set equal to 100°C at this point. Water took a while to decrease (it used to reach about 0,030 % vol before the introduction of the first standard).
- Close valve number 4, number 0 and 1. In this way the sample was limited in a small volume size (between 0 and 1).
- Remember to change the inlet value = 15000 (smaller value) and the outlet min = 10000, in order to let the instrument better control the cavity pressure and so let the pressure difference between inner and outer

environment be high enough to drive the flow through the set up. In this way the cavity pressure oscillated around 19.99-19.92 Torr at the most, without decreasing too much and at the same time the flow could not decrease too much.

- Then the evacuation between 4 and 1 could start with in addition a heating set to 180°C.
- Wait 30 minutes. Write down pressure value from the pressure gauge; stop the evacuation, remember to set down to 100°C and stop heating.
- *Put on cooling (liquid nitrogen bath) under the sample trap.*
- Open valve number 1 to let the sample enter the sample trap.
- Wait at least 20 minutes. Then take off the cooling, put on a heat=100°C; close valve number 3 and wait to reach 100°C.
- After reaching 100°C, wait 5 minutes to let it stabilize.
- Before introducing the sample into the analyzer, remember to re-set inlet=16000 and outlet min= 17000. Write down the pressure from the pressure gauge: it used to be about 2.4-2.6 E² mBar, which means in terms of volume about 5 ml/min.
- Open valve 4 and introduce the sample.
- Keep monitoring the trend of the concentrations for at least 50 minutes.
- Stop the experiment. Close valve 4, open valves 3 and 0 and evacuate the whole system before the next standard analysis.
- Evacuate the line through P, S, 4 and 0 for 5- 10 minutes then close P and evacuate the other way between valves 3, 2, 1, and 0 for other 10 minutes.
- Stop evacuation and intruduce of the next standard through the extraction line.
- Trap the sample between valves 0 and 1 and start a new experiment.

Each of the standard gases was measured at least 4 times. These experiments were exploited in order to calibrate the analyser and to test the first calibration.

Results:

Up to this point the measured concentrations from dry gases seemed to be quite reliable: they showed the same behaviour (as in *Figure 5. 3*) for all the blank experiments: they reached a constant value over time, even if higher than the expected one. The water vapour remains constant as expected. The first calibration could be considered reliable and it also seemed to work quite well, decreasing the values.

Figure 5. 3 shows one of the many attempts of these blank experiments.

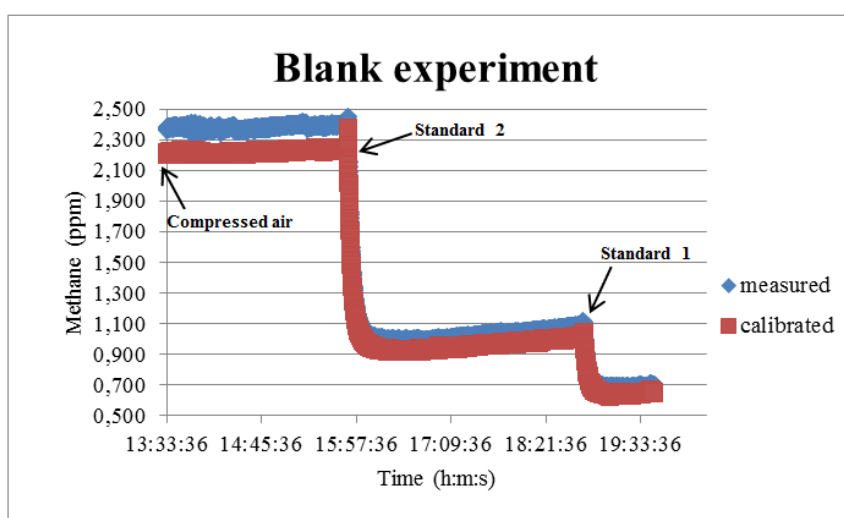


Figure 5. 3 The curve shows one of the many attempt for these kind of experiments. From the left to the right is showed the respective experiment for each standard. Black arrows indicate the introduction of the standard gas sample, followed by fifty minutes monitoring and by an evacuation (except for the last standard, where the experiment has been directly interrupted after the monitoring).

5.1.2 Air Free Ice (AFI) experiments

Regarding these kind of tests since a noticeable amount of water was expected from the glass vessel after the ice melting, the water vapor trap was equipped with a cooling system in order to increased the capture capacity of its filler material (the lower the temperature, the higher the trap property; see 4.3.2 *Memory effect* paragraph). Initially, it consisted in submerging the water vapor

trap into a bath made by ethanol and dry ice, which is able to decrease the temperature till about -70°C .

Procedure:

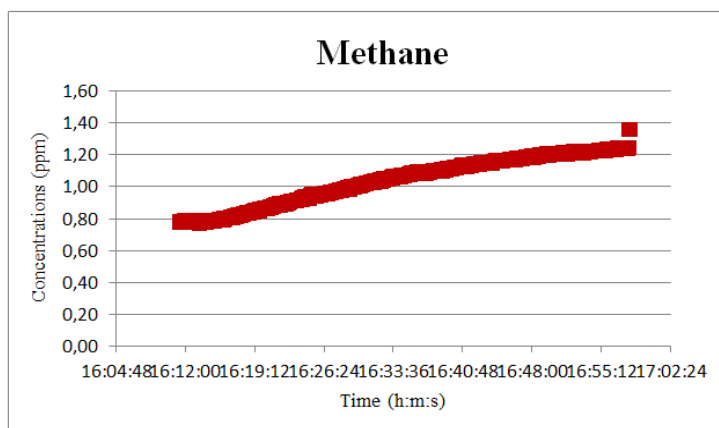
- Evacuation of the system (till at least $E-3$ mbar).
- Stop evacuation. Heat from 180°C to 100°C .
- Introduction of standard 2 (the closest to real samples in terms of concentrations). Let it running in continuous flow for 20 minutes, till the concentrations reach stable values.
- In the meantime clean glass vessel with ethanol and put it in the freezer (with some water to make fake ice or an air free ice).
- Prepare bath with ethanol + dry ice for glass vessel in order to prevent the melting of the ice while it was attaching to the extraction line
- Prepare bath ethanol + dry ice for water vapor trap.
- Write down concentrations values, flow.
- Change inlet=15000 and outlet min. = 10000 ready for evacuation.
- Close 0 (with real sample I did not need to close 0).
- Close 1, 2 and 4 and start to evacuate. Heat = 180°C . Close standard bottle.
- Put on glass vessel + ethanol-dry ice pot under it.
- Open valve 2 to let evacuate also between valves 2 and 1.
- Give 25 minutes for evacuation (should reach 10^{-3} mBar on the pressure gauge).
- After 25 minutes stop evacuation. Write down the value.
- Set Heat = 100°C and turn in off.
- *Put ethanol-dry ice pot under water trap.*
- Take off ethanol-dry ice bath from the glasse vessel.
- Put a warm water pot under glass vessel to help the melting.

- Put liquid nitrogen under sample trap. The liquid nitrogen is here employed in order to cool the sample trap, thus to increase the absorption power of the filler (HaeySep) material, allowing the sample capture.
- Let it melted. Once it is completely melted, write down the P from Pressure gauge (about 4.5-3.9 E2 mBar).
- Close valve 3. Stop cooling the sample trap.
- Turn on the heat = 100°C. Wait to reach 100°C. The heat was employ for the mixing of the sample before the introduction.
- Change inlet = 16000 and outlet min = 17000 few second before the introduction.
- Introduce the sample, open valve 4.
- Monitor the concentrations.

Results:

Despite numerous attempts, all of these experiments failed after few minutes of concentrations' monitoring due to anomalous trends, i.e. too high values and in continuous increase, especially for CO₂ (over 9000 ppm), but also for CH₄ (see figure below), *Figure 5. 4*. Regarding the water: it was properly removed at the water vapor trap.

Such a problem occurred only when the glass vessel was introduced into the extraction line and the dry gas sample was replaced with the air sample coming from the piece of ice.



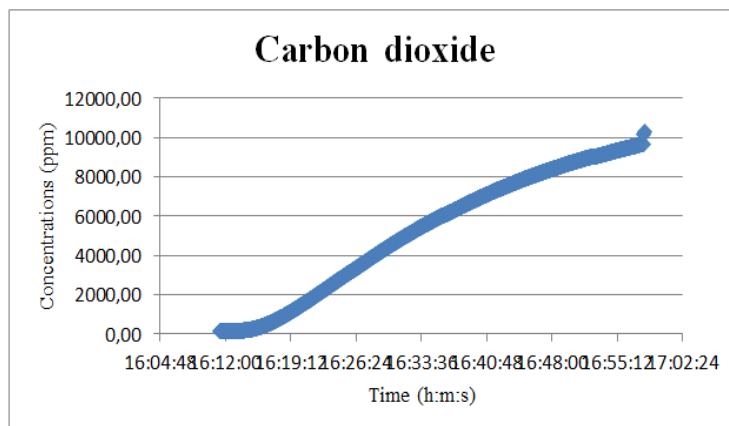


Figure 5. 4 The anomalous trends for both CO₂ and CH₄ are showed above, as result of one of the many attempts for AFI experiments. The experiment was interrupted due to unreliable values.

This represented a huge issue, since it was exactly the kind of measurement that I needed for real procedure and it did not allow reliable values yet. In some cases it was found that the glass vessel was not properly sealed and that the excess CO₂ consequently could be produced by the dry ice-ethanol bubbling under glass vessel. However, even after fixing this point on the extraction line, the issue did not disappear.

Ultimately, the final correction has been to replace the ethanol-dry ice bath under the water vapor trap, with a liquid nitrogen bath (able to cooldown to -198°C) in order to increase the trap capacity of the filler material (glass beads) and in such way to capture most of the CO₂ at the water trap point, removing the source of the mysterious issue.

Therefore, to get reliable measurements for the calibration, one last blank experiment has been repeated with this last procedure improvement. This adjustment seemed to be necessary: removing CO₂, even if without a specific and clear reason, I also avoided its influence on CH₄ values; the instrument was able to provide reliable measurements for CH₄. The success of such new protocol has also been confirmed by a further AFI experiment, which finally provided satisfactory values (red curve in *Figure 5. 6*).

Later, methane values for real sample experiments have been calibrated considering the closest Blank experiment to the real procedure (the one with liquid nitrogen under the water vapor trap). Therefore, the final calibration for methane in the actual samples, was derived plotting the expected values versus the corrected ones from the last Blank experiment (*Figure 5. 5*):

$$CH_4calibrated = (CH_4corrected - 0,1452) / 1,0507$$

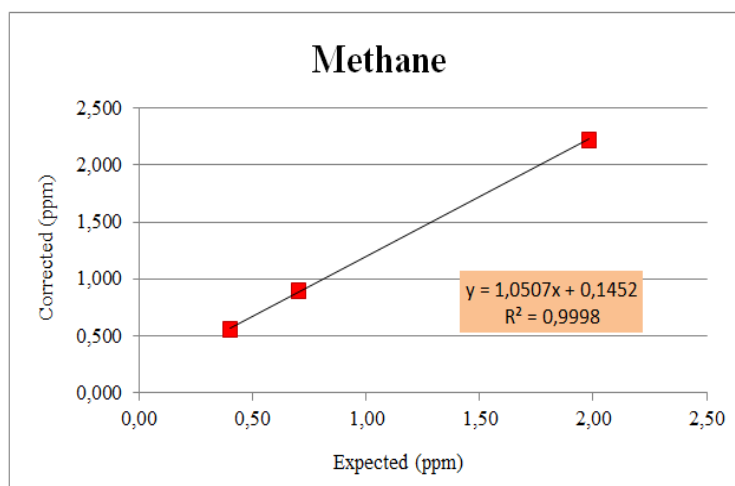


Figure 5. 5 The final calibration for real samples, based on the last Blank experiment with three standards.

Figure 5. 6 shows the calibration applied to the methane measurements of the last AFI experiment.

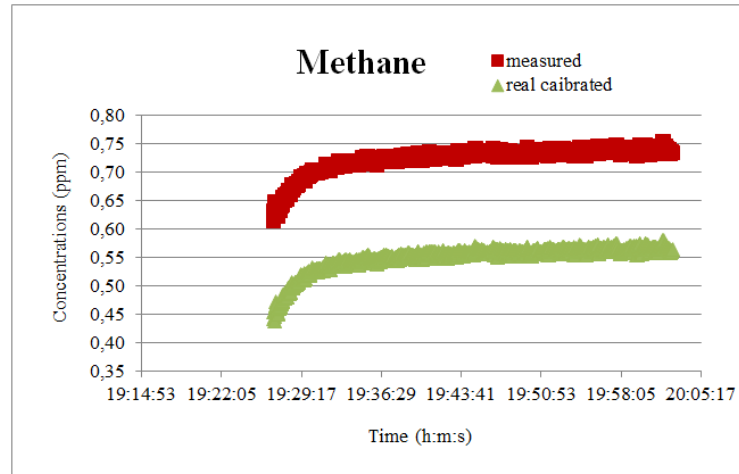


Figure 5. 6 Red curve shows the measurements from the last AFI experiment, in which the concentrations increased till stabilizing around a constant value over time; Green curve show the values with final calibration.

5. 2 Analytical accuracy

These calibrations series also enabled to derive the uncertainty of the system, i.e. the *analytical accuracy*.

In order to calculate that, another calibration was derived based on the last three Blank experiments values for methane. Therefore, the standards expected and the corrected concentrations were plotted (*Figure 5.7*).

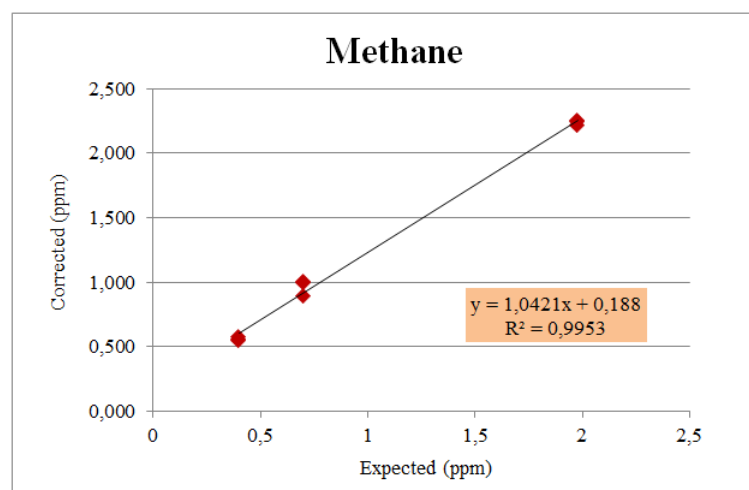


Figure 5. 7 Calibration made in order to have an idea about the uncertainty of the system. It was derived on the basis of the three last Blank experiments, the best ones.

The slope and the offset values from the linear equation have been applied to calibrate each standard for each blank experiment, as followed:

$$(CH_4_{corrected}-0.188)/1.0421 = (ppm)$$

Ultimately, a *standard deviation* between the three calibrated values, for each standards, has been calculated and employed in this final formula:

$$\sqrt{(\sigma_{st1})^2 + (\sigma_{st2})^2 + (\sigma_{c.air})^2}$$

Where σ_{st1} σ_{st2} and $\sigma_{c.air}$ are the standard deviations for standard 1, standard 2 and compressed air respectively.

$$\sigma_{st1} = 0.0138 \text{ ppm}$$

$$\sigma_{st2} = 0.0604 \text{ ppm}$$

$$\sigma_{c.air} = 0.0165 \text{ ppm}$$

The analytical accuracy resulted equal to 0.0641 ppm, i.e. **64,1 ppb**.

6. Real sample experiments

6.1 Cutting the ice

Eighteen ice sticks, of 55 cm length, have been collected from the Priorparken deposit, the institutes ice core storage facility on the outskirts of Copenhagen and transported to our institute for the cutting process and eventually the analyses (*Figures 6. 1 and 6. 2*).



Figure 6. 1 View from the huge freezer ice storage in Priorparken



Figure 6. 2 Another view of the ice boxes's piles.

Once drilled, the 304 m core of the Eurocore project was divided in 55 cm pieces and, further cut into sections in parallel to the core axis. Samples have been sent to several institutes among others the University of Bern where they were analyzed for the methane concentration published in Blunier in 1993. My samples come from a project for nitrate analyses that never took off. They come from the same depth level as those published in Bunier et al., 1993. Samples on a given depth level were separated at most by 55 cm, corresponding to a difference of age of about 2 years and hence a negligible difference in composition of the air-bubbles (Blunier et al. 1993). The specific ice samples to analyse, has been established by my supervisor, in order to reconstruct a methane record for the last 1000 years. Furthermore, the ice sample sizes were derived from the air sample amount that I employed during the calibration tests, which was about 5 ml (i.e. 2.6-2.4 E2 mBar of pressure within sample trap).

Hence, since a kilogram of ice can provide at most 100 ml of air, I needed about 50 grams of ice sample in order to get about 5 ml of sample volume to analyse. A workstation was specifically set up for the cutting, inside a freezer kept at -27°C. Each sample was cut from the top of an ice stick for a length of about 6-7 cm (*Figure 6. 3*); subsequently it was cleaned along each side with a microtome knife, then re-measured and weighed (*Figure 6. 4*). In order to obtain a constant amount of gas I have tried to cut ice samples of similar sizes. However, the span is quite with differences up to a factor of two. The prepared samples have been stored in a chest freezer at -20°C until the beginning of the experiments.

The ice sticks have been taken from Box n°:

- 1008 (9 A 23): sticks/samples n° 159 - 179 - 198 - 215 - 233 – 270 – 287
- 1076 (9 A 22): sticks/samples n° 305 - 323 - 341- 392 - 421
- 2007 (9 A 21): sticks/samples n° 440 - 451 - 478 - 494 - 513 - 531



Figure 6. 3 a picture of me cutting the ice stick.



Figure 6. 4 an example of ice sample sizes.

The following table (*Table 8*) shows the samples with the respective age, depth and weight.

Table 8 Each sample with the respective age (years AD), depth (m) and weight (g)

N° Samples	Gas age yr AD	Depth (m)	Weight (g)
159	1907	88	56
179	1864	99	49
198	1817	109,45	46
215	1775	118,8	51
233	1734	128,7	49
270	1651	149,05	54
287	1605	158,4	42
305	1555	168,3	51
323	1510	178,2	45
341	1466	188,1	49
392	1335	216,15	43
421	1254	232,1	43
440	1210	242,55	50
451	1165	248,6	39
478	1114	263,45	40
494	1075	272,25	38
513	1025	282,7	58
531	974	292,6	64

6.2 Daily calibration

A calibration was conducted every day before measuring the first sample of the day, in order to confirm that the Picarro provided reliable measurements.

Therefore, each morning both standard 1 and standard 2 were introduced in continuous flow and the concentrations were monitored for about 40 minutes.

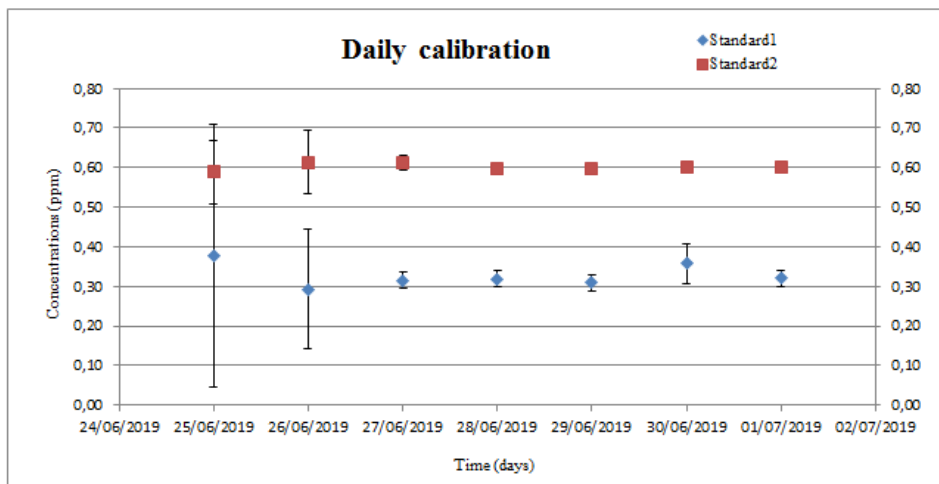


Figure 6. 5 Standard 1 in blu dots and standard 2 in red squares, monitored everyday for daily calibration.

Except for the first two measurement days, values are quite constant, thus reliable, as shown by *Figure 6.6* and *Table 9* below.

Table 9 Standard daily measurements before the first sample of the day. The unit of measure is still ppm.

	Standard 1	Standard 2
I day	0,38 ± 0,33	0,59 ± 0,08
II day	0,29 ± 0,15	0,61 ± 0,08
III day	0,32 ± 0,02	0,61 ± 0,02
IV day	0,32 ± 0,02	0,60 ± 0,01
V day	0,31 ± 0,02	0,60 ± 0,01
VI day	0,36 ± 0,05	0,60 ± 0,01
VII day	0,32 ± 0,02	0,60 ± 0,01

6.3 Real procedure

Daily calibration

- Evacuation of the system for about 30 minutes (till reaching at least E^{-3} mBar). Heat =180°C. Valve 5 is turned towards laboratory air meanwhile (it is closed).
- Stop evacuation.
- Evacuate the line through P for 5 minutes.
- Stop evacuation. Heat=100°C.
- Introduction of the standard 1. Turn valve 5 towards the extraction line (open).
- Let it running in continuous flow for about 40 minutes, i.e. till the concentrations do not reach a stable value.
- In the meantime clean the glass vessel with ethanol and cool down it in freezer with the sample inside.
- Stop Standard 1 continuous flow measurements.

- Close valves 4 and 0. Close Standard 1 bottle.
- Set heat=180°C.
- Change inlet=15000, out min=10000.
- Turn off the rotary pump, open S. Evacuation of the line through valve P, the one that connects the standard bottles. Then stop evacuation. Rotary pump on and evacuate for 10 minutes the other line through 4, 0 and S (open valve 4, 0). The vacuum should reach about E^{-3} mBar.
- Close 0.
- Stop evacuation and keeping 0 closed.
- Heat=100°C
- Open Standard 2 bottle and let it in continuous flow for other 40 minutes.
- Prepare bath with ethanol + dry ice for glass vessel, in order to better preserve the ice sample during the connection to the extraction line.
- Prepare liquid nitrogen for water vapor trap and sample trap.
- Write down concentrations, flow values and stop the monitoring.

Sample extraction

- Change inlet=15000 and outlet min. = 10000. Close valves 1, 2 and 4 and start to evacuate. Heat = 180°C.
- Evacuation with rotary pump off. Close standard 2 bottle.
- Put on glass vessel with the ice sample and the ethanol-dry ice bath under it (*Figure 6. 7*). The glass vessel is sealed also by an O-ring between its body parts equipped with a plastic clamp. It is connected



Figure 6. 6 Ethanol-dry ice bath under the glass vessel

to the extraction line via U-torr connection.

- Open valve 2 to let evacuate also between 2 and 1, including glass vessel.
- Turn on rotary pump. Give 25 minutes for evacuation (it should reach E^{-3} mbar on the pressure gauge).
- Then stop the evacuation. Write down the pressure value from the pressure gauge.
- Set Heat =100°C and turn it off.

Trapping the excess water vapor and collecting the sample air

- Put liquid nitrogen under water trap. Put liquid nitrogen under sample trap. In both cases the purpose, as explained for AFI experiments, is to cool down those sections and increased their trap capacity for the capturing of water vapor and sample respectively.
- Take off ethanol-dry ice bath from the glass vessel and put a warm water pot under it in order to help the melting (40-45°C), see *Figure 6. 8*.

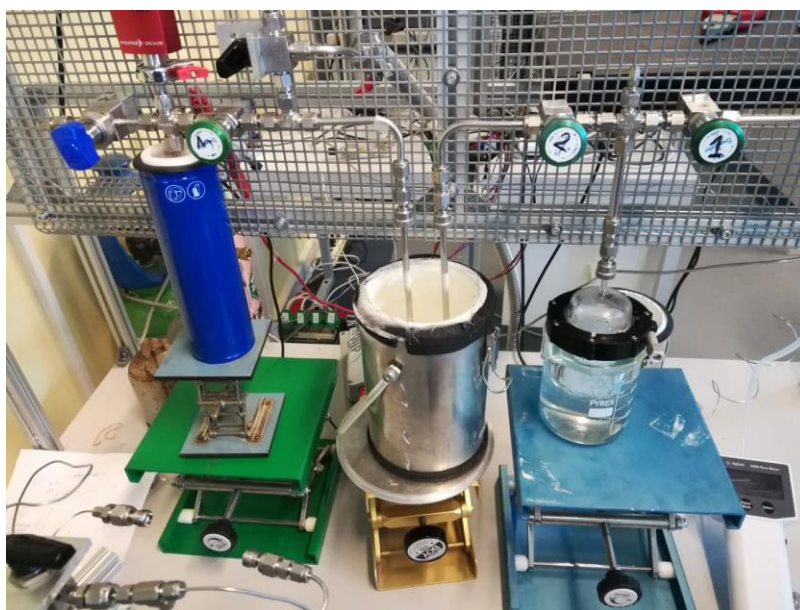


Figure 6. 7 view of the whole extraction line during the ice melting and the extraction of the air sample.

- Let it melt. (it takes more or less 10 minutes). The released air while ice sample is melting, flows towards the sample trap characterized by a significant amount of water. The excess water vapor is trap, together with the CO₂ amount, at the water vapor trap.
- Once it is completely melted, remove the warm water pot (to not generate further pressure).
- Put ethanol bath under glass vessel for refreezing the ice and allow a complete release of air bubbles. Wait the re-freezing time.
- Close valve 3. Stop cooling sample trap.
- Turn on the heat=100°C. After reaching 100°C, wait other 5 minutes.
- Write down the P reached from the pressure gauge; that represents the sample pressure, thus it allows to derive the sample volume before that I will analyse.
- Change inlet=16000 and outlet min= 17000 few second before the introduction.
- Introduce the sample: open valve 4.
- Monitor the concentrations for about 50 minutes (*Figure 6. 9*), considering the early ten minutes for the stabilization. Take the last 20 minutes for deriving the average value.

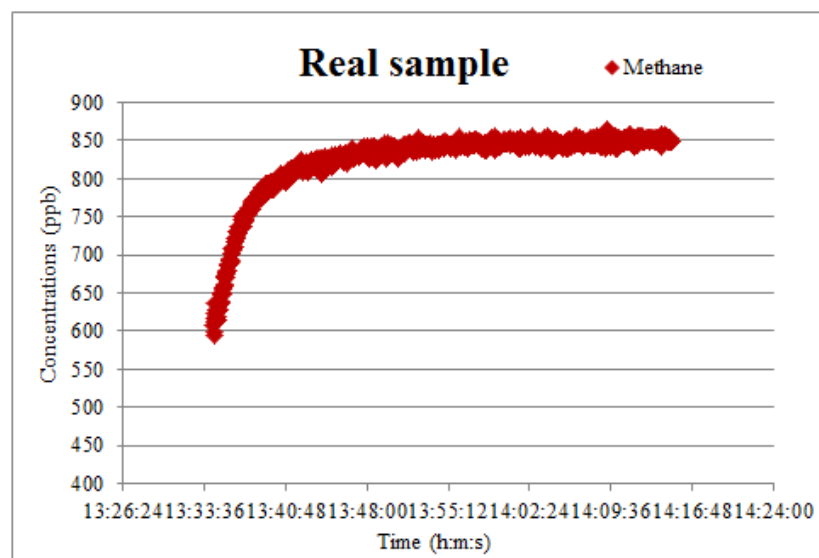


Figure 6. 8 An example of real sample monitoring. This is the case of sample n° 478.

While a sample is running through the instrument, it is already possible to prepare most of the set up for the next sample.

- Keeping closed valve 3, evacuate the line from 3 and 2 with rotary pump turn off.
- The glass vessel is disconnected, cleaned and cooled down into the freezer with the new sample.
- The water trap tube is switched with an other one that it has been already kept cleaned with pure nitrogen flow. This switch is necessary to measure many samples in a day. It would take too long to be cleaned and completely empty from water only through a system evacuation.
- At the end of the experiment evacuate for 30 minutes the rest of the extraction line, between valve 3 and S, with rotary pump on.
- Start a new experiment.

7. Results from Eurocore samples

The measurement protocol with ice core samples is explained above (paragraph 6.3). Here, the results about methane concentrations from Eurocore samples are presented.

Table 10 The measurement result from Eurocore ice samples. The depth and Gas age are provided by (Blunier et al. 1993). The variance for my measurements can be derived from the standard deviation, and is equal to 16 ppbv.

Sample n°	Gas age yr AD	Weight (g)	Depth (m)	Methane (ppbv)
159	1907	56	88	971
179	1864	49	99	842
198	1817	46	109,45	782
215	1775	51	118,8	733
233	1734	49	128,7	714
270	1651	54	149,05	684
287	1605	42	158,4	794
305	1555	51	168,3	736
323	1510	45	178,2	722
341	1466	49	188,1	684
392	1335	43	216,15	756
421	1254	43	232,1	695
440	1210	50	242,55	725
451	1165	39	248,6	726
478	1114	40	263,45	848
494	1075	38	272,25	716
513	1025	58	282,7	696
531	974	64	292,6	704

7.1 Comparison with published results

Blunier et al. in 1993 provided the atmospheric methane trend of the last 1000 years, confirming the mean pre-industrial methane atmospheric level around 700 ppbv and the increasing trend from the end of the XVIII century. The analyses were carried out in gas chromatography from two laboratories: one in Bern,

where the gas was extracted with a dry extraction method, the other in Grenoble, where a melt extraction technique was exploited. I presented below the results from both the laboratories, since they are of similar quality, that I used for the comparison with my measurements. See *Table 11* and *Table 12* for Bern and Grenoble results respectively. The analytical accuracy for Bern's measurements, derived from a standard calibration with Air Liquide (1200 ± 100 ppbv of CH₄), is ± 40 ppb. Whereas for Grenoble the calibration with Messer Griessheim (980 ± 30 ppbv of CH₄) yielded an uncertainty of ± 28 ppbv. An intercalibration of the standard gases used by the two laboratories showed an agreement better than ±5 ppbv. Therefore it is possible to assume that the absolute uncertainty of the standard gases used in Bern and Grenoble corresponds to ± 30 ppbv.

Table 11 The measurement results from Bern analysis in 1993, with respective depth and Gas age. In red are shown the most deviant values compared to my measurements. The variance for Bern's measurements is ±20 ppbv.

Sample n°	Gas age yr AD	Depth (m)	Methane (ppbv)
159	1907	89,2	996
179	1864	99,3	870
198	1817	110,1	808
215	1775	118,9	803
233	1734	128,8	753
270	1651	148,8	740
287	1605	158,4	730
305	1555	168,8	763
323	1510	178,2	761
341	1466	188,4	690
392	1335	216,1	692
421	1254	233,5	694
440	1210	242,9	743
451	1165	252,4	763
478	1114	263	738
494	1075	272,3	711
513	1025	283	722
531	974	292,6	714

Table 12 The measurement results from Grenoble analysis in 1993, with respective depth and Gas age. In red are shown the most deviant values compared to my measurements. The variance for Grenoble's measurements is ± 40 ppbv.

Sample n°	Gas age yr AD	Depth (m)	Methane (ppbv)
159	1905	89,6	968
179	1865	99,1	896
198	1842	104,5	818
215	1815	110,5	754
233	1774	119,2	765
270	1690	139	774
287	1652	148,6	750
305	1603	158,8	722
323	1557	168,4	781
341	1508	178,6	728
392	1467	188,2	727
421	1357	211,5	688
440	1320	219,2	749
451	1304	222,7	733
478	1253	233,7	656
494	1210	243	774
513	1168	251,9	752
531	/	292,6	/

Observing the graph below (*Figure 7. 1*) both the general methane trend and the compatibility between my results and the ones from Blunier analyses is evident. There is a systematic offset according to which my data is up to 50 ppbv lower, except for three heavier anomalous values. Noteworthy is the fact that some of the differences might be explained considering the different standard calibrations that have been employed within the two studies, which also bring to different analytical accuracies.

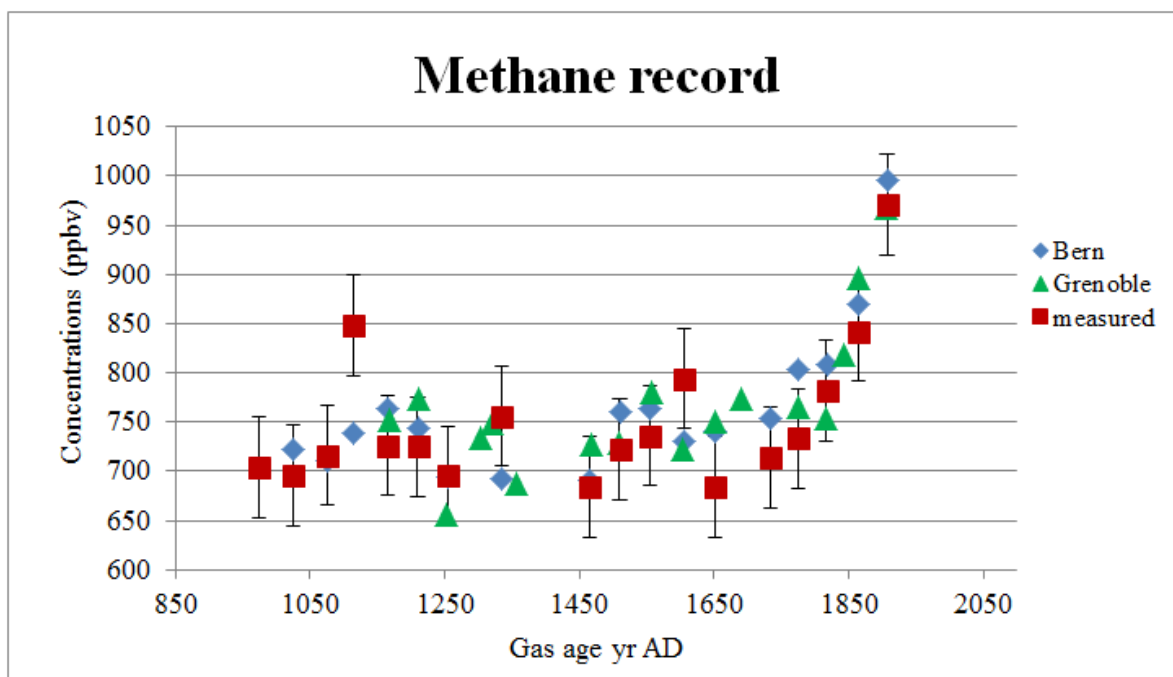


Figure 7. 1 Methane record from Eurocore ice samples both from published data and my results. In blue Bern's results, in green Grenoble's values, both measured by gas chromatography; in red squares my values, taken through the Picarro G1301 analyzer.

8. Discussion

In this section, I discuss my results and possible causes for the concentrations offset comparing to Blunier's CH₄ record.

The very general trend of the CH₄ record is evident and consistent with previously published data by Blunier (*Figure 7.2*), with a roughly stable level before 1750 (AD) and a large growth from the beginning of the nineteenth century, most likely linked to the increase in greenhouse gas emissions by human activity. The overall average around 700 ppbv for the time interval 1000-1750 AD, previously declared by Blunier and even by older studies, is here confirmed.

The characteristics of the records obtained from the two analysis are very similar, as confirmed by the linear comparison showed by *Figure 8.1* below.

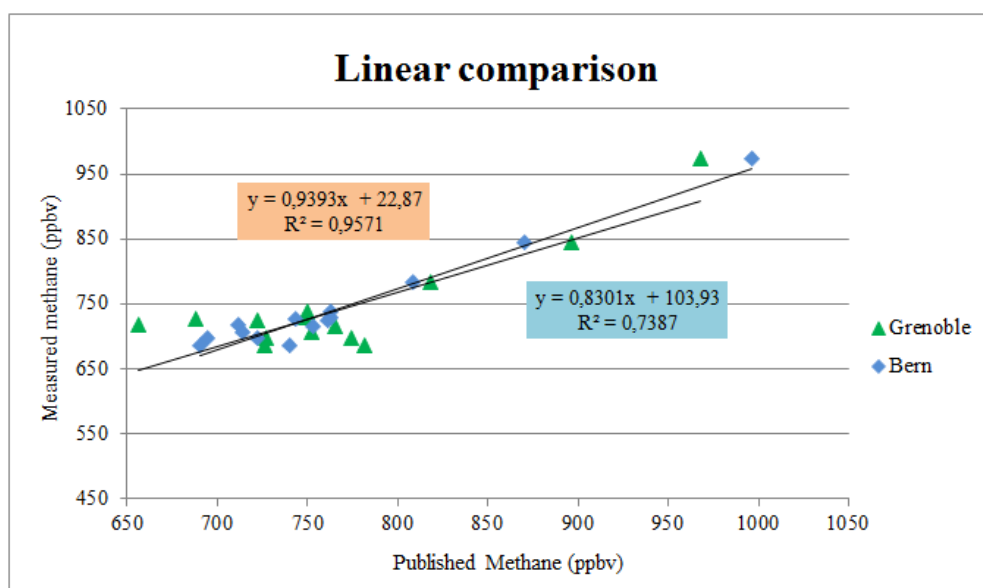


Figure 8. 1 Measured values are plotted versus published values making a linear comparison. I excluded the three outliers in order to have a better fit. The relation is quite good, especially for Bern values.

One could immediately observe that the mean pre-industrial level is the same within the error ranges. Anyway, Blunier's values are constantly heavier than mine, also for the most recent samples. Furthermore, it is possible to identify three anomalous cases, especially for Bern's values, in which my measurements tend to be slightly heavier (samples 287, 392 and 478, respectively deviate of about 64, 64 and 110 ppbv).

Regarding my values, the error range, i.e. the uncertainty on the y axis, represented on the graph (*Figure 7. 1*), is based on a three dry gases calibration, and it is equal to ± 51 ppb. Such uncertainty generally works very well for the rest of the samples; moreover, considering the actual uncertainty of my system, which is ± 64 ppbv, it is quite reasonable that 3 of my measurements (actually just two of them stand out of 64 ppbv error range), among a total of 18, do not perfectly fit with the published results of 1993. An analytical uncertainty of 64 ppbv means that about 68% of my results need to be within 64,1 ppbv, and that up to 1/3 of the data outside the uncertainty range is still acceptable.

A possible explanation for these three "outliers" might be that there has been a pre-analysis contamination (poor ice preservation in situ and/or during sample preparation) or during analysis itself. This cannot be the case for the old Bern/Grenoble samples, since they have been measured in two laboratories on different samples with different extraction techniques. These values are quite deviant that the best thing would be to repeat the measurements in order to verify their validity, which was not possible for me due to the time restriction of my stay in Copenhagen. Another explanation, may also recall the fact that the ice in situ could be fractured and that therefore some modern air had infiltrated downwards through the fractures, reaching higher depths. Then, due to refreezing and sublimation processes, such fractures have been sealed again and no evidence of them has remained within the ice.

The consistent offset along y axis, i.e. the fact that Blunier's values are constantly heavier, might be explain considering the difference between the Gas Chromatograph and the most recent and advanced Picarro analyzer. Gas

Chromatography relies on a separation column and a FID detector (Flame Ionization Detector) which burns the gas flow and gives an electric answer based on the particles' amount. This technique relies on the different interaction between the components of a complex mixture and the stationary phase of the column. Within the GC different molecules of a gas mixture are separated by their affinity to the stationary phase which allows the transport by a carrier gas of different components along the column, with times that differs based on the boiling temperature, if a temperature ramp is necessary to accelerate the components' elution, or just on the different affinity with the stationary phase. Generally, in case of heating, molecules that are smaller, lighter and with lower boiling temperatures, such as methane, will be released first. The risk is that two molecules characterized by a very similar boiling temperature will be released more or less at the same time and in this way identified as the same molecule, i.e. as unique electric signal. Since the Picarro relies on the optical absorption phenomenon, which is very characteristic and occurs at a specific wavelength for each molecule, it is also able to act as a "filter" (which is not the case of the FID) giving back only the analytical signal of the molecule of interest (based on its typical transition energy). In such a way the analytical signal is cleaner and, likely, lower than that of the FID, which is not equally selective. Alternatively, it could also just be calibration offsets between the results: for instance an error in my calibration or the fact that the three records derived from three different standard calibration processes (a three standards calibration in my case, whereas a calibration based on a unique standard gas for Blunier). Indeed, part of the considerations for my analysis has been which point calibration to use; I employed different methods: some of them have been done with dry gas through the entire process, others having also an ice surface to interact with. Ultimately, we chose the one resulted from the last calibration experiment (the last blank experiment), which followed the closest procedure to the real one. Moreover, it should be accounted that everything was analysed only once in my case, whereas in Bern's laboratory generally two samples, from the same depth level, were measured (samples from a given depth level, as I

already mentioned, separated at most by 55 cm, corresponding to a difference of air age that is negligible). Hence, it is reasonable to think that my samples could be further measured and consequently results improved.

The slight offset along x axis can be related to the fact that I have worked on samples from the same ice core of Blunier but not exactly the same, because he used GC, which is a destructive technique. Thus, I have utilized the closest samples that I could (more or less 50 cm), which bring a negligible difference in composition of the air-bubbles.

Obviously, for accurate and completely reliable measurements one must consider that during the whole project some issues have been encountered. First of all, the presence of leaks which were located especially on the extraction line and which have been fixed as much as possible, tightening or switching the screws of interest; since further I assumed that the system was sufficiently tight and isolated to provide reliable measurements. Another meaningful issue was connected to the memory effect of the sample trap and subsequently also due to the water vapor trap, which affected discrete measurements of the early experiments, yielding anomalous values for both CO₂ and CH₄. Such problem has been removed installing a heating system and a liquid nitrogen bath under the sample trap and the water vapor trap respectively. One last important consideration must be done regarding the flow effect and its complex relation with methane concentrations. My final values could be quite different as result of such unsolved issue, which was not possible to remove due to its complexity and which need to be further investigated. However, as already explained, it is incorporated within the standard calibration too, thus it actually represents a constant presence which can be neglected here; methane values might be slightly different, but always following the same trend, which is the most valuable result.

9. Conclusions

This thesis project presented the development of discrete measurements for methane mixing ratio in air bubbles trapped within the ice of Summit, Central Greenland. The crucial point was the employing of the Picarro G1301 analyzer and its respective experimental set up in order to reconstruct the atmospheric methane record for 974-1907 AD, with a more advanced technology than the gas chromatography utilized for the same analysis by Blunier, in 1993. Here some disadvantages of the past analytical methods have been overcome, such as the problem with limited number of samples by using low sample volume of about 5 ml and, for instance, the incredible response time of measurements, provided by fast spectroscopic scans, immediately converted into concentration values. Moreover, the Picarro analyser compared to the GC is a non-destructive method which enables multiple measurements of the same sample; for instance, connecting two non-destructive instruments together and analysing the same sample by both of them. However, the main advantage provided by the Picarro is the fact that it is more selective, as it acts like a filter, thus it is able to yield more accurate measurements than GC. Additionally, since the Picarro G1301 can perform measurements of methane and water vapor at the same time, this system avoids the need to dry the sample air stream before the analysis, as established in GC. The water vapor content need in any case to be reduced at most around 0.05%, and this simply occurs within the water vapor trap on the extraction line.

The Picarro analyzer enables to get excellent accuracy in measurements but it is extremely important that it is able to keep steady conditions both for cavity pressure and temperature during analysis. Particularly, for the purpose of this work the instrument needed to operate at the lowest of the two possible cavity pressure, i.e. 20 Torr, in order to produce, for an extended time, sufficient pressure difference between the Picarro and the sample container to produce a reasonable sample flow. I have tested the pressure dependence of the methane measurements for this low-pressure condition and found a pressure effect equal

to 5% per Torr. Detected pressure offsets were taken into account in the final evaluation.

Other issues stood out during the discrete experiments: besides the leaks' presence, which has been detected and fixed, and the memory effect of sample trap, also corrected with the heating system, the most meaningful problem regarded the flow influence (paragraph 4.3). Due to its rather complex effect, neither absolute nor relative, it could not be easily removed.

The experimental system was calibrated with three different standard gases (methane conc. of 1980, 400 and 700 ppbv respectively for compressed air, standard 1 and standard 2) through many experiments (Blank and AFI), which encountered part of the issues and finally allowed to derive an analytical uncertainty of ± 64 ppbv; slightly higher than the one of Blunier (± 40 ppbv) but still reasonable.

Eighteen samples from Eurocore ice core were analysed, employing a wet extraction for the air sample, trapping it within the sample trap and finally intruding it into the CRDS cavity. These air samples covered a time range of about 1000 years. The atmospheric methane record is here confirmed by my results: it is characterized by a mean pre-industrial level around 700 ppbv (Blunier et al. 1993) and a recent anthropogenic increase with the rise of modern human activity. Additionally, without considering the three anomalous results (regarding samples 287, 392 and 478), most likely contaminated, the pre-industrial variations² in the range of 70 ppbv, previously defined by Blunier et al., are also verified here. 20 to 60% of these variations should be explained by changes in the oxidising capacity of the atmosphere, whereas the larger contribution comes from changes in methane emissions linked both to natural sources, i.e wetlands and to an early menmade influence (Blunier et al. 1993).

Therefore, my results can be considered quite satisfying, as they resemble the values published by Blunier et al, but it is paramount to consider that the flow effect still affects the results, which would reproduce the same trend but with

² By concentration fluctuations during the pre-industrial period we mean those which characterized the time interval from 900 to 1700 AD.

slightly different values. Further works are necessary in order to better understand its relation with concentrations and to find out an effective way to remove it. For instance, what can be done for testing the flow effect could be to measure the flow effect at different flows, as I have already done, but in this case for multiple concentrations of methane, in order to see how it behaves at different levels.

10. Acknowledgments

This thesis's project comes at the end of a five-years journey which has meant to me much more than a simple university career. The years of Padua were for me, more than anything else, a life experience; the first adventure far away from home and my family, the conquest of independence and for the first time facing the solitude. They have been the greatest growth's opportunity I could ever wish for, which is why I will never be sufficiently grateful to my parents and my family. Thank you mum and dad for your endless support, for the values you have always taught me and for the example of honesty, humility and generosity you give me every day. Thanks to my brother Emanuele for being a constant stimulus for me since I was a child and to my twin-sister Sara for bringing joy and happiness to my life; no matter how far we are, you always made me feel loved. A huge thanks is for my grandmothers: Esterina and Luigia; you have been the most powerful example of strength and resilience and I will never forget how much you taught me.

Thanks to my uncles Luigi and Sergio, to my aunt Pierangela and my cousin Pierpaolo: you have always made me feel your support and love.

For the success of this work, I would like to thank, first of all, the Professor Luca Capraro for accepting to be my inner supervisor, and thus giving me the opportunity to live this great experience abroad. Thank you for supporting me from Italy and for guiding me on this journey since my bachelor degree. Thanks to the professor Patrizia Ferretti, for the availability, the attention and the advice she has always reserved for me. Thanks to doc. Sara Pizzini from Venice's CNR-ISP for her availability and her technical support during these last weeks.

I would like to thank the professor Thomas Blunier for giving me his confidence and this unique opportunity to work in his laboratory. Thank you Thomas, during those months I had the privilege to experience what "research" really means: attempts at attempts, trying and retrying, maybe not having results but never give up. It is never a failure. Even non-results lead to progress and this is

certainly the greatest teaching I could have received. I would like to thank Jesper too. I would not be here “mentally healthy” without your guidance, your help and your extraordinary patience. Thanks to Janani and David for being such good mates during my Danish time, I miss you guys! Thanks to all the Neils Bohr institute’s people, for making me feel comfortable since the first day and for the amazing and stimulating atmosphere you always showed me.

There are three more special people left from my Danish experience I would like to thank: my flatmates! Thank you Roger, Kalle and Tanya: I will never forget our delicious brunches and how much you did help me.

Thanks to all my friends and mates of a lifetime. To all my volleyball teammates and all the friends from Padova I had the pleasure to meet: feeling your loyalty and support all these years fills my heart with joy and gratitude. Thanks for being here with me today to celebrate a such important success. You make me feel so so lucky!

Finally, I would like to thank Francesco, my boyfriend, the most amazing, passionate and inspiring person I have ever met. I will always thank you for your sincere support and love.

Ringraziamenti

La realizzazione di questa tesi si pone alla fine di un percorso di cinque anni che ha significato per me molto più di una carriera universitaria. Gli anni di Padova son stati, più di qualsiasi altra cosa, un'esperienza di vita; la prima avventura fuori casa, lontano dalla mia famiglia, la conquista di un'indipendenza e, allo stesso tempo, per la prima vera volta, la solitudine. Sono stati la più grande opportunità di crescita che potessi desiderare, per questo so che non potrò mai essere sufficientemente grata ai miei genitori, e alla mia famiglia. Mamma e papà grazie perché mi avete sempre sostenuta, sopportata e, quando è servito, anche lasciata andare ad inseguire i miei sogni. Grazie per i valori che mi avete trasmesso, per quei no che solo dopo anni ho saputo apprezzare; grazie per l'esempio di onestà, umiltà e generosità che mi date ogni giorno. Grazie Manu, perché anche se non sei il classico fratellone estroverso e baci e abbracci, sei sempre stato un importante punto di riferimento per me; colui che fin da piccola dovevo riuscire a sorprendere e a far ridere. Quindi grazie per essere da sempre, per me, un costante stimolo. Grazie Sara, sei la persona che mi accompagna da sempre, ancor prima di essere nata; inutile dire quanto tu sia stata importante per me in tutti questi anni. Ti ho lasciata sul più bello, lo so, ma ti ringrazio per avermi compresa e supportata ogni giorno anche a distanza; senza di te la mia vita sarebbe profondamente noiosa, lo sai. Grazie nonna Ester, mi hai cresciuta e coccolata; grazie per le lasagne e i ravioli migliori del mondo, per le tue storie, e le preghiere prima degli esami. Non smetterai mai di insegnarmi qualcosa, me lo ribadisci ogni giorno. Grazie nonna Luigina, perché anche se non sei qui, sei stata il mio angelo custode in questi anni. Nei momenti di difficoltà non ho mai smesso di rivolgermi a te. So che saresti stata orgogliosa di me.

Grazie ai miei zii Luigi, Pierangela e Sergio e a mio cugino Pierpaolo; anche da lontano siete sempre riusciti a farmi sentire il vostro affetto e il vostro sostegno.

Per la riuscita di questo lavoro, vorrei ringraziare, innanzitutto il professor Luca Capraro per aver accettato il ruolo di supervisor interno, e avermi così dato la

possibilità di vivere questa grande esperienza nel mondo della ricerca. Grazie per avermi sostenuta a distanza e per avermi accompagnata in questo percorso fin dalla laurea triennale. Grazie alla professoressa Patrizia Ferretti, per la disponibilità, l'attenzione e i consigli che mi ha sempre riservato. Un grazie speciale alla dottoressa Sara Pizzini del Centro Nazionale delle Ricerche – Istituto di Scienze Polari (CNR-ISP) di Venezia, per la sua disponibilità e il supporto tecnico di queste ultime settimane.

Un immenso grazie al professor Thomas Blunier, per la sua fiducia e per avermi dato l'opportunità di lavorare nel suo laboratorio, di provare nel concreto cosa significa “ricerca”: tentativi su tentativi, provare e riprovare senza perdere la fiducia; che non c'è fallimento, ma che anche i non-risultati portano ad un progresso e questo è il più grande insegnamento che potessi ricevere. Grazie a Jesper, non sarei qui “mentalmente sana” senza la tua guida, il tuo aiuto e la tua pazienza. Grazie a Janani e David per esser stati dei buoni compagni di viaggio, mi mancate ragazzi! Grazie a tutta la gente del Neils Bohr Institute per l'atmosfera stimolante e di sincera condivisione con la quale mi avete accolta fin dal primo giorno. Dei miei mesi danesi ci sono ancora tre persone speciali che vorrei ringraziare: i miei coinquilini! Grazie Roger, Kalle e Tanya: non dimenticherò mai i nostri brunch domenicali, i pic-nic al parco e quanto mi siete stati d'aiuto.

Grazie alle mie amiche e amici di una vita, cresciuti con me nella nostra semplice realtà di paese, piccola ma genuina. È così bello poter festeggiare oggi con voi questo traguardo, e rendersi conto degli importanti percorsi che ciascuno di noi ha intrapreso. Grazie alla mia compagna di avventure Giorgia, ormai sempre lontana ma vicina al mio cuore. Grazie ad Alessandra per l'amica speciale che si è rivelata in questi anni. Grazie a Maddalena per i continui spunti di riflessione e la tua sincera amicizia da anni. Grazie a Monica, la mia amica di sempre, per aver condiviso con me prima Padova e ora anche questa esperienza danese. Ai miei amici del Leo, grazie perché nonostante non ci si veda più tanto spesso quando ci si ritrova è come se nulla fosse cambiato. Grazie in particolare

a Lorenzo e Matteo, per le risate, per il mio Paffu in Kenya e per le sessioni di studio insieme.

Grazie alla gente di Padova che in questi anni ha rappresentato la mia quotidianità: alle mie coinquiline, diventate presto amiche: Veronica, Caterina, Elisabetta, Hasna, Anna e Deborah, grazie per il tempo trascorso insieme e le serate di trash televisivo; grazie ai miei cari Geoamici: Eleonora (la mia spalla destra), Censo, Alberto, Luca, Giorgia e a tutti gli altri che con me hanno vissuto la realtà dello studente geologo: le escursioni, i campi di rilevamento, le carte, i microscopi, i laboratori, gli esami infiniti di questi ultimi due anni. Ebbene ragazzi, non sarebbe stato lo stesso senza di voi!

A tutte le mie amiche pallavoliste, dalle prime in assoluto, con le quali ho imparato a giocare e ormai da anni care amiche: Chiara, Eleonora e Valentina. Grazie alla mia ammi Francesca, che sa sempre ascoltarmi e consigliarmi, e sulla quale so di poter sempre contare. Grazie al volley Fratte che in questi anni patavini è stato per me come una seconda famiglia. Sarò per sempre grata alla pallavolo per aver portato tutte voi nella mia vita.

Infine grazie a te, Francesco. Per l'esempio di passione e entusiasmo che mi dai ogni giorno, in tutto quello che fai. Per spronarmi sempre a non accontentarmi, ma a cercare ciò che mi rende felice. Grazie per essere cresciuto insieme a me, per avermi saputo aspettare e aver sopportato con pazienza la distanza. Ora so che non importa dove, ma insieme.

Grazie Amigo mio, per avermi appoggiata, anche stavolta, in questa grande sfida. Sei la cosa migliore che potesse capitarmi.

11. References:

- Battle. 1996. 'Battle1996.Pdf'.
- Bender, M. 1985. '© 1985 Nature Publishing Group'.
- Beng, Tan Sooi, Eugene van Erven, and Timothy Wiles. 2006. 'The Playful Revolution: Theatre and Liberation in Asia'. *Asian Folklore Studies* 53 (1): 175. <https://doi.org/10.2307/1178566>.
- Blake, Donald R., and F. Sherwood Rowland. 1988. 'Continuing Worldwide Increase in Tropospheric Methane , 1978 to 1987 Author (s): Donald R . Blake and F . Sherwood Rowland Published by : American Association for the Advancement of Science Stable URL : [Http://Www.Jstor.Org/Stable/1700583](http://www.jstor.org/stable/1700583) REFERENCES Lin' 239 (4844): 1129–31.
- Blunier, T, J Schwander, J Barnola, T Despertis, B Stauff, and D Raynaud. 1993. 'GEOPHYSICAL LETTERS , with a Standard Deviation of about 7 Years [Schwander et Al ., and Data Pairs' 20 (20): 2219–22.
- Chen, H., J. Winderlich, C. Gerbig, A. Hofer, C. W. Rella, E. R. Crosson, A. D. Van Pelt, et al. 2010. 'High-Accuracy Continuous Airborne Measurements of Greenhouse Gases (CO₂ and CH₄) Using the Cavity Ring-down Spectroscopy (CRDS) Technique'. *Atmospheric Measurement Techniques* 3 (2): 375–86. <https://doi.org/10.5194/amt-3-375-2010>.
- Coachman, L K, E Hemmingsen, and P F Scholander. 1956. 'Te L L u S' 2826 (1956). <https://doi.org/10.3402/tellusa.v8i4.9042>.
- Delmas. 1980. 'Delmas1980.Pdf'.
- Fuchs, A., Schwander, J., and Stauffer, B. 1993. 'Instrument and Methods A New Ice Mill Allows Precise Concentration Determination of Methane and Most Probably Also Other Trace Gases in the Bubble Air of Very Small Ice

- Samples'. *Of Glaciology* 39 (131): 199–203.
- Heuberger, M S. 1955. 'Journal of Glaciology'.
- Jouzel, J. 2013. 'A Brief History of Ice Core Science over the Last 50 Yr'.
Climate of the Past 9 (6): 2525–47. <https://doi.org/10.5194/cp-9-2525-2013>.
- Jouzel, Jean, Liliane Merlivat, and Claude Lorius. 1982. 'Deuterium Excess in an East Antarctic Ice Core Suggests Higher Relative Humidity at the Oceanic Surface during the Last Glacial Maximum'. *Nature* 299 (5885): 688–91. <https://doi.org/10.1038/299688a0>.
- Lassey, K. R., G. W. Brailsford, A. M. Bromley, R. J. Martin, R. C. Moss, A. J. Gomez, V. Sherlock, et al. 2010. 'Recent Changes in Methane Mixing Ratio and Its ¹³C Content Observed in the Southwest Pacific Region'. *Journal of Integrative Environmental Sciences* 7 (SUPPL. 1): 109–17. <https://doi.org/10.1080/19438151003621441>.
- Lelieveld, J O S, Paul J Crutzen, and Frank J Dentener. 1998.
'H:\BROMR\DIVERSE\Litteratur\artikler\drivhusgasser\metanChanging Concentration, Lifetime and Climate Forcing of Atmospheric Methane'.
Tellus B 50 (2): 128–50.
- Morgan, V.I. 1997. 'Site Information and Initial Results from TI . Deep Ice Drilling on Law Dome , Antarctica', 3–10.
- Ommen, Van. 2007. 'ICE CORE METHODS / Methane Studies' 4 (2000).
- Paterson, W.S.B, and R M Koerner. 1977. 'From the Devon Climatic Record', no. April 1977. <https://doi.org/10.1038/266508a0>.
- Petit, J R, J Jouzel, D Raynaud, N I Barkov, J.-M Barnola, I Basile, M Bender, et al. 1999. 'Climate and Atmospheric History of the Past 420,000 Years from the Vostok Ice Core, Antarctica The Recent Completion of Drilling at Vostok Station in East'. *Nature* 399: 429–36. www.nature.com.

- Physics, Applied. 2008. 'A Cavity Ring-down Analyzer for Measuring Atmospheric Levels of Methane , Carbon Dioxide , and Water Vapor' 408: 403–8. <https://doi.org/10.1007/s00340-008-3135-y>.
- Report, This, H A S Been, Cleared For, Public Release, N O Restrictions, A R E Imposed, I T S Use, Approved For, Public Release, and Distribution Unlimited. n.d. 'THIS REPORT HAS BEEN DELIMITED'.
- Schmidt, Ehhalt &. 1978. 'Sources and Sinks of Atmospheric Methane' 116: 3–4.
- Schwander, J, J Barnola, C Andrie, M Leue, and A Lvdin. 1993. 'The Age of the Air in the Firn and the Ice at Summit , Greenland' 98 (02): 2831–38.
- Schytt, V. 1950. 'THE NORWEGIAN-BRITISH-SWEDISH EXPEDITION , 1949-52 ANTARCTIC SUMMARY OF THE GLACIOLOGICAL WORK PRELIMINARY REPORT'. *Journal of Glaciology*, no. November.
- Sower T., Ed Brook, David Etheridge, and Martin Wahlen. 1997. 'An Interlaboratory Comparison of Techniques for Extracting and Analyzing Trapped Gases in Ice Cores 4 Were Consistent at the of O2 Measurements Showed of N2 Measurements Were Five Laboratories Analyzed The'. *Journal of Geophysical Research* 102 (C12): 26,527-26,538.
- Stowasser, C, A D Farinas, J Ware, D W Wistisen, C Rella, E Wahl, E Crosson, and T Blunier. 2014. 'Author Copy' c (cc). <https://doi.org/10.1007/s00340-013-5528-9>.
- Stowasser, Christopher. 2013. 'Continuous Greenhouse Gas Measurements from Ice Cores', no. May.
- Taylor, K.C. 1993. 'Taylor K. C. Electrical Conductivity Measurements from the GISP2 and GRIP Greenland Ice Cores.Pdf'.
- Yiou, F, G M Raisbeck, S Baumgartner, J Beer, C Hammer, S Johnsen, J Jouzel, et al. 1997. 'Beryllium 10 in the Greenland Ice Core Project Ice Core at

Summit , Greenland Abstract . Concentrations of the Cosmogenic Isotope
Have Been Measured in More Component of • ^{10}Be Retained Origin of
Robe Concentration Variations Is Changes in Precipitation Ra'. *Journal of
Geophysical Research* 102 (C12): 26,783-26,794.

J.Jouzel (2013). A brief history of ice core science over the last 50 yr. *Clim.
Past*, 9, 2525-2547.